

Biomaterial Interfaces Division

Room B117-119 - Session BI2+AS+HC+SS-MoM

Energy Transfer and Light Induced Phenomena in Biologic Systems

Moderators: Morgan Alexander, University of Nottingham, UK, Tobias Weidner, Aarhus University, Denmark

10:40am **BI2+AS+HC+SS-MoM-8 Electrochemically Conducting Lipid Bilayers: Q-Lipid-Containing Membranes Show High in-Plane Conductivity Using a Membrane-on-a-Chip Setup**, U. Ramach, TU Wien, Austria; J. Andersson, IST Austria; Markus Valtiner, TU Wien, Austria

The light-driven reactions of photosynthesis as well as the mitochondrial powersupply are located in specialized membranes containing a high fraction of redox-active lipids. In-plane charge transfer along such cell membranes is recurrently thought to be facilitated by the diffusion of redox lipids and proteins.

Using a membrane on-a-chip setup, we show here that redox-active model membranes can sustain surprisingly high currents (mA) in-plane at distances of 25 nm. We also show the same phenomenon in free-standing monolayers at the air-water interface once the film is compressed such that the distance between redox centers is below 1 nm. Our data suggest that charge transfer within cell walls hosting electron transfer chains could be enabled by the coupling of redox-lipids via simultaneous electron and proton in-plane hopping, similar to conductive polymers. This has major implications for our understanding of the role of lipid membranes, suggesting that Q-lipid-containing membranes may be essential for evolving the complex redox machineries of life.

[1] U. Ramach, J. Andersson, R. Schöfbeck and M. Valtiner, *Iscience* 26 (2), 2023.

11:00am **BI2+AS+HC+SS-MoM-9 Light Responsive Cyclic Peptide Polymer Nanomaterials**, O. Atoyebi, M. Beasley, W. Maza, M. Kolel-Veetil, A. Dunkelberger, Kenan Fears, US Naval Research Laboratory

Cyclic peptides are capable of self-assembling into supramolecular peptide nanostructures, via hydrogen bonding along the backbone of the peptide rings. To improve upon this molecular architecture, we designed and synthesized cyclic peptide polymers by covalently linking the cyclic peptides into a linear polymer chain, and demonstrated the conformation of the polymer chain could be transitioned from an unfolded state into rigid, peptide nanorods by varying solution pH. Here we present an alternate way to control the self-assembly via photo-isomerization. We capitalize on azobenzene's photo-actuable nature using a di-carboxylic acid azobenzene to covalently crosslink the cyclic peptide rings into a linear cyclic peptide polymer via terminal amines present in the ring. Self-assembly of the cyclic peptide nanotube occurs by exposing the polymerized cyclic peptide to ultraviolet radiation causing a trans- to -cis transition of the azobenzene and thus assembling the cyclic peptide nanotube. Furthermore, we fluorescence donor/acceptor pairs can be displayed from these materials, at highly controlled separation distances, to alter the optical response of these materials as a function of polymer conformation.

11:20am **BI2+AS+HC+SS-MoM-10 Programmable Biomimetic Light-Harvesting Systems based on Strong Coupling of Synthetic Peptides and Dye-Functionalised Polymer Brushes to Plasmon Modes**, Graham Leggett, University of Sheffield, UK

Excitation transfer in molecular photonic materials is dominated by incoherent hopping processes; consequently, exciton diffusion lengths are short (~10 nm) placing severe constraints on device design. A grand challenge for the past two decades has been to discover how to achieve efficient long-range transfer of excitation in molecular systems. We have developed a new approach to the design of materials for solar energy capture that combines biomimetic design, inspired by structures used in photosynthesis, with strong light-matter coupling.

Photosynthetic pigment-protein light-harvesting antenna complexes (LHCs) from plants and bacteria are strongly coupled to the localised surface plasmon resonances (LSPRs) in arrays of metal nanostructures leading to the formation of macroscopically extended excited states. Modelling of data indicates that the coupling results from linear combinations of plasmon and exciton states. For example, wild-type and mutant LH1 and LH2 from *Rhodobacter sphaeroides* containing different carotenoids yield different coupling energies; the methods of synthetic biology enable strong light-matter coupling to be programmed.

However, proteins are not suitable for putative applications of molecular photonic materials. Instead, we have designed programmable biomimetic pigment-peptide and pigment-polymer antenna complexes, in which surface-grafted peptide and polymer scaffolds organise excitons within localised surface plasmon resonances to achieve strong light-matter coupling. In these systems, delocalised excited states (plexcitons) extend across at least 1000s of pigments. In synthetic peptide and protein systems, we find that the plasmon mode couples to states not seen under weak-coupling, providing evidence for the formation of macroscopically-extended excited states that facilitate coherent transfer of excitation across long distances. In pigment-polymer systems, the dye concentration in the film can be increased to ~2M, significantly exceeding the concentration of chlorophyll in biological light-harvesting complexes, by optimisation of the polymer grafting density and the dye-scaffold coupling chemistry. Fitting of spectra for these plexcitonic antenna complexes yields Rabi energies up to twice as large as those achieved with biological LHCs. Moreover, synthetic plexcitonic antenna complexes display pH- and temperature-responsiveness, enabling active control of strong plasmon-exciton coupling via regulation of the polymer conformation.

These biomimetic quantum-optical brush systems offer great promise for the design of new types of molecular photonic device.

Laboratory-Based Ambient-Pressure X-ray Photoelectron Spectroscopy Focus Topic

Room B116 - Session LX+AS+HC+SS-MoM

Laboratory-Based AP-XPS: Advances in Instrumentation and Applications

Moderators: Sylwia Ptasinska, University of Notre Dame, Heath Kersell, Oregon State University

8:20am **LX+AS+HC+SS-MoM-1 Instrumentation for Electron Microscopy and Spectroscopy in Plasma Environment**, Andrei Kolmakov, NIST-Gaithersburg

INVITED

Plasma-assisted processes are of principal importance for modern semiconductors microfabrication technology, catalysis, environmental remediation, medicine, etc. Understanding the chemical and morphological evolutions of the surfaces and interfaces under a plasma environment requires *operando* metrologies that have a high spatial, temporal, and spectroscopic resolution. Combining the APXPS system with ambient pressure scanning electron microscopy would, in principle, meet these needs. Here we review the status of the field and discuss the prospective designs as well as application examples of ambient pressure scanning electron microscopy and spectroscopy for *in situ* analysis and processing of the surfaces under plasma environments

9:00am **LX+AS+HC+SS-MoM-3 Scienta Omicron HiPPLab - A Lab-based APXPS Instrument for Probing Surface Chemical Reactions**, Peter Amann, Scienta Omicron, Germany

Investigating reaction intermediates, oxidation states, solid-liquid interfaces and buried interfaces under near ambient pressure conditions is highly desired in materials science applications. Ambient pressure X-ray photoelectron spectroscopy (APXPS) is a powerful method to investigate the chemical nature of surfaces and interfaces and has undergone a tremendous improvement in the last years. The development of the HiPP analysers allowed to overcome the one bar pressure regime without using pressure separating membranes. [1] [2]

During the past decade, increased attention has been shown to laboratory based APXPS system solutions, which is motivated by the 24/7 access capability and possibility for highly customized sample environments. Drawing on extensive experience in the fields of photoelectron spectroscopy, UHV technology, and system design, Scienta Omicron has designed the HiPPLab as an easy-to-use system that encourages user creativity through flexibility, modularity and an innovate chamber design.[3] It combines a state-of-the-art HiPP analyser with a high flux, variable focus X-ray source. Multiple options complement the HiPPLab offer, including a gas reaction cell, a preparation chamber, laser heating, or options for mass-spectroscopy. Using automated gas-flow controllers, experiments can be conducted in a controlled way. Future upgrade possibilities are given.

The HiPP-3 analyser features a 2D detector allowing for spatial resolved measurements with customer proven results down to 2.8 μm resolution. The swift acceleration mode allows for high electron transmission without

Monday Morning, November 6, 2023

applying a sample bias. A sophisticated pre-lens design in which efficient pumping between two close-by apertures is implemented, allows dragging out corrosive gases or moisture, which would otherwise be detrimental to the instrument.

In this presentation, I will give an overview on our APXPS product portfolio focusing on laboratory based solutions and present application examples.

[1] Amann, et al. *Review of Scientific Instruments*, 2019 90(10)

[2] Takagi, et al. X-ray photoelectron spectroscopy under real ambient pressure conditions. *Applied Physics Express*, 2017, 10(7), 8–11.

[3] Scienta Omicron HiPPLab <https://scientaomicron.com/en>

9:20am **LX+AS+HC+SS-MoM-4 Using Microheaters for Time-Resolved APXPS and Correlated ETEM**, **Ashley Head**, Brookhaven National Laboratory; **B. Karagoz**, Diamond Light Source, UK; **J. Carpena-Nuñez**, Air Force Research Laboratory; **D. Zakharov**, Brookhaven National Laboratory; **B. Maruyama**, Air Force Research Laboratory; **D. Stacchiola**, Brookhaven National Laboratory

With a rise in the number of lab-based APXPS systems, these instruments afford an opportunity to continue the development of multimodal and correlated capabilities for more comprehensive information of reactions at surfaces. Here I will discuss the methods of using an ETEM commercial microheater for collecting APXPS data on the same sample under identical conditions. A specialized holder was fabricated to use commercial microheaters on MEMS chips in a lab-based APXPS instrument. The rapid heating of the microheater enables a time-zero for collecting APXPS data with a time resolution of 500 ms. Proof-of-principle measurements following the oxidation and reduction of a Pd film demonstrate correlative experiments with TEM. The specialized holder was fabricated with the possibility of dosing gases locally to the sample surface while confined by a graphene membrane. Using the gas lines, the Pd film was oxidized under a partial pressure of air (~0.4 mbar). Overall, using this microheater in APXPS offers chemical information complementary to structural changes seen in ETEM. The rapid heating enables new opportunities in time-resolution and increased pressure for APXPS experiments.

9:40am **LX+AS+HC+SS-MoM-5 NAP-XPS Instrumentation Came a Long Way - Where Will Applications Lead Us from Here?**, **P. Dietrich**, **F. Mirabella**, **K. Kunze**, **O. Schaff**, **Andreas Thissen**, SPECS Surface Nano Analysis GmbH, Germany

INVITED

Over the last fifty years significant developments have been done in photoelectron spectroscopy instrumentation and thus opened new fields of application. Especially XPS or ESCA developed into the most important standard surface analytical method in many laboratories for surface and materials characterization.

For the last fifteen years XPS under near ambient pressure conditions (NAP-XPS) has gained significant attention. Although invented as a laboratory method it initially started to grow at synchrotrons. The development of more efficient and sensitive electron analyzers and high-brilliance monochromated laboratory X-ray and UV sources running at pressures of up to 100 mbar finally brought it back to the individual laboratories. The reasons are the availability of individual infrastructure for sample preparation and handling, safety regulations and easier access to measurement time on a daily basis. Nowadays the vast majority of instruments worldwide are laboratory-based.

It opened the method XPS to liquids, solid-liquid interfaces, gas-solid-interfaces, gas-liquid-interfaces and many more. The development of instrumentation followed the important applications and besides the "active" components, mainly excitation sources and electron analyzers, a lot of developments have been done in the fields of sample environments, sample handling, system setup and automation and combination with other techniques and even in quantification of data. There are only a few applications left where experiments at synchrotron based beamlines and end stations offer the only solution.

The market driving applications nowadays are catalysis, electrochemistry, behaviour of liquid phases, biological samples and surface chemistry. Along these applications this presentation will show the existing instrumentation, discuss its limits and the perspective for near future developments to further increase the user base of laboratory based NAP-XPS systems to turn it into an integral part of the large routine analysis community.

10:40am **LX+AS+HC+SS-MoM-8 Evolution of Metal-Organic Frameworks in the Presence of a Plasma by AP-XPS and IRRAS**, **J. Anibal Boscoboinik**, Brookhaven National Laboratory and State University of New York at Stony Brook; **M. Ahmad**, Stony Brook University/Brookhaven National Laboratory; **M. Dorneles de Mello**, Brookhaven National Laboratory; **D. Lee**, Johns Hopkins University; **P. Dimitrakellis**, University of Delaware; **Y. Miao**, Johns Hopkins University; **W. Zheng**, University of Delaware; **D. Nykypanchuk**, Brookhaven National Laboratory; **D. Vlachos**, University of Delaware; **M. Tsapatsis**, Johns Hopkins University

INVITED

Zeolitic imidazolate frameworks (ZIF), a class of metal-organic frameworks, are promising materials for various applications, including the separation and trapping of molecules and catalysis. Recent work has shown that exposure to plasma can result in the functionalization of the framework for tailored applications. This talk will report in-situ plasma studies of ZIF-8 as a model system. We will study the framework's evolution in the presence of N₂, O₂, and H₂ plasmas by combining lab-based ambient pressure XPS and infrared reflection absorption spectroscopy.

11:20am **LX+AS+HC+SS-MoM-10 Surface Degradation and Passivation in Perovskite Solar Cells**, **Wendy Flavell**, The University of Manchester, UK

INVITED

There is an urgent requirement to make better use of the 120,000 TW of power provided by the Sun, by using it to generate power, or by using its energy directly to make useful chemical feedstocks. Around the world, there is an explosion of research activity in new systems for harvesting solar energy, including solar cells based organometal halide perovskites. Issues of key importance are the interfacial energy level line-up of the cell components, and the influence of the surface properties of these materials on charge separation in the devices. Indeed, the deployment of perovskites in solar cells is currently limited by their high reactivity and rate of surface oxidation. Thus, a key problem is to develop an understanding of the interface chemistry of solar heterojunctions in order to develop passivation strategies. I show how a combination of techniques including near-ambient pressure X-ray photoelectron spectroscopy (NAP-XPS) and hard X-ray photoelectron spectroscopy (HAXPES) may be used to investigate surface ageing and the surface degradation reactions[1-7], chemical composition as a function of depth[4,5], and to develop passivation strategies for perovskite solar cell heterojunctions[2,3,5-7].

References

1. J C-R Ke, A S Walton, A G Thomas, D J Lewis, *et al.*, *Chem Commun* **53**, 5231 (2017).
2. J C-R Ke, D J Lewis, A S Walton, B F Spencer, *et al.*, *J Mater Chem A*, **6**, 11205 (2018).
3. C-R Ke, D J Lewis, A S Walton, Q Chen, *et al.*, *ACS Applied Energy Materials* **2**, 6012 (2019).
4. B F Spencer, S Maniyarasu, B P Reed, D J H Cant *et al.*, *Applied Surface Science* **541**, 148635 (2021).
5. S Maniyarasu, J C-R Ke, B F Spencer, A S Walton *et al.*, *ACS Applied Energy Materials* **13**, 43573 (2021).
6. S Maniyarasu, B F Spencer, H Mo, A S Walton *et al.*, *J Mater Chem A*, **10**, 18206 (2022).
7. D Zhao, T A Flavell, F Aljuaid, S Edmondson *et al.*, *ACS Applied Materials and Interfaces*, submitted.

Surface Science Division

Room D136 - Session SS1+HC-MoM

Electrochemistry

Moderators: Jan Balajka, TU Wien, Sefik Suzer, Bilkent University, Turkey

8:20am **SS1+HC-MoM-1 Surface Inhomogeneities and Ordering Phenomena of (Pr,Ba)CoO_{3-δ} Thin Film Electrocatalysts Induced by High Temperatures and Oxygen Partial Pressures**, **David Mueller**, **M. Giesen**, **T. Duchon**, **C. Schneider**, Forschungszentrum Jülich GmbH, Germany

Complex transition metal oxides are used ubiquitously in (electro-)catalysis, ternary and quaternary compounds of the perovskite structure showing especial promise for increasing the efficacy of a plethora of redox reactions. The perovskite structure ABO₃ being able to accommodate a huge range of elements on both A- and B-site allows to tune the electronic and physicochemical properties and tailor those towards a certain catalytic application by careful design of the chemistry. This rational design paradigm has led to the identification of simple descriptors that offer structure-

property-activity predictions. These descriptors, mostly derived from the electronic states near the Fermi level, can, for example, be elucidated through X-Ray absorption (XAS) or photoemission spectroscopy.¹

The catalyst surfaces, however, are dynamic in technologically relevant conditions. Design rules thus have to consider structural, chemical and electronic rearrangements at the surface during catalysis or catalyst processing. Adding to this complexity, spatial inhomogeneities may arise from decomposition pathways that are not found in the bulk, and occur on length scales that can not be resolved by standard electrochemical or spectroscopic techniques.

Here, we investigate (Pr,Ba)CoO_{3-δ} (PBCO) as a prototypical example material that exhibits both promising catalytic properties towards the oxygen evolution reaction in solid electrochemical cells² as well as a rich structural and chemical complexity depending on oxygen content.³ Exposing epitaxial thin films grown by pulsed laser deposition to elevated temperatures and oxygen partial pressures typically present in operation, we could identify severe chemical rearrangements at the nanoscale using X-Ray absorption photoelectron microscopy (X-PEEM). We employ principal component analysis on the spatially resolved XAS spectra of all constituents to unambiguously identify correlations of chemical and electronic inhomogeneities.^{4,5} Even though PBCO has been found to be thermodynamically stable in the cubic phase over a wide range temperature and oxygen partial pressures in the bulk, our data suggests a Cahn Hillard type decomposition process confined to the surface after mere hours of exposure. The decomposition products show a considerable lateral inhomogeneity of both A-site chemistry and the electronic structure at the surface, emphasizing that activity descriptors derived from this through spatially averaging techniques have to be heavily scrutinized.

¹J. Suntivich *et al.*, *Science* **334**, 1383–1385 (2011); ²A. Grimaud *et al.*, *Nat. Commun.* **4**, 2439 (2013); ³C. Frontera, *Chem. Mater.*, **17**, 5439–5445 (2005); ⁴M. Giesen *et al.*, *Thin Solid Films* **665**, 75–84 (2018). ⁵D. N. Mueller *et al.*, *J. Phys. Chem. C* **125**, 2021, 10043–10050

8:40am SS1+HC-MoM-2 Understanding the Influence of Electrolyte and the Buried Interface on the Stability of Hybrid Systems: A Spectro-Electrochemical Approach, Tom Hauffman, N. Madelat, B. Wouters, A. Hubin, H. Terryn, Vrije Universiteit Brussel, dept. Materials and Chemistry, Belgium

The stability of the interface between (organic) coatings and metal (oxides) is of crucial importance for the durability and efficiency of hybrid structures in numerous applications, e.g. in food packaging, automotive, ... This interface is a challenging zone to analyze: from both sides covered with micro- to millimeter thick layers, surface sensitive spectroscopic techniques cannot unravel its characteristics in a non-destructive way. Moreover, the change of this interface due to environmental influences remains challenging to reveal.

In this work, we propose the use of a combined electrochemical and spectroscopic method: Odd Random Phase Multisine Electrochemical Impedance Spectroscopy in combination with Infrared Spectroscopy in a Kretschmann geometry. This fusion allows to correlate the global electrochemical characteristics of the system – such as water uptake and ion diffusion – with enhanced interfacial information.

The concept of this approach is proven on ultrathin PAA and PMMA layers on aluminium oxide¹, clearly elucidating the surface sensitivity of the Kretschmann geometry and unravelling the enhanced adhesion effect of water on short time scales.

The combined characterization tool has been employed on “industrial-like” organic coatings on model engineering metals. Here, the influence of water uptake, the possibility to make a distinction between water ingress and water diffusion, the influence of both species on delamination and corrosion and the influence of the tuned buried interface will be presented^{2,3,4}.

1. Pletincx S. *et al.*, An in situ spectro-electrochemical monitoring of aqueous effects on polymer/metal oxide interfaces, *Journal of Electroanalytical Chemistry* **848** (2019).
2. Wouters B. *et al.*, Monitoring initial contact of UV-cured organic coatings with aqueous solutions using odd random phase multisine electrochemical impedance spectroscopy, *Corrosion Science* **190** (2021).
3. Madelat N. *et al.*, Differentiating between the diffusion of water and ions from aqueous electrolytes in organic coatings using an

integrated spectro-electrochemical approach, *Corrosion Science* **212** (2022).

4. Madelat N. *et al.*, An ORP-EIS approach to distinguish the contribution of the buried interface to the electrochemical behaviour of coated aluminium, *Electrochimica Acta* **455** (2023).

9:00am SS1+HC-MoM-3 Controlling CO₂ Reduction and Electrocatalysis Reactivity Using Alloy and Polymer-modified Electrodes, Andrew Gewirth, University of Illinois at Urbana Champaign

INVITED

This talk addresses the reactivity associated with CO₂ and nitrate electroreduction. Electrodeposition of metals from plating baths containing 3,5-diamino-1,2,4-triazole (DAT) as an inhibitor yields highly porous materials exhibiting enhanced activity for electrochemical reactions. Electrodeposition of Cu or CuAg and CuSn, alloy films from such plating baths yields high surface area catalysts for the active and selective electroreduction of CO₂ to multi-carbon hydrocarbons and oxygenates. Alloy films containing Sn exhibit the best CO₂ electroreduction performance, with the Faradaic efficiency for C₂H₄ and C₂H₅OH production reaching nearly 60 and 25%, respectively, at a cathode potential of just –0.7 V vs. RHE and a total current density of ~300 mA/cm². *In-situ* Raman and electroanalysis studies suggest the origin of the high selectivity towards C₂ products to be a combined effect of the enhanced destabilization of the Cu₂O overlayer and the optimal availability of the CO intermediate due to the Ag or Sn incorporated in the alloy. Sn-containing films exhibit less Cu₂O relative to either the Ag-containing or neat Cu films, likely due to the increased oxophilicity of the admixed Sn. A related effect is found for nitrate reduction on alloy-modified Cu electrodes. Modification of the Cu electrode with certain polymers yields substantially enhanced CO₂ reduction reactivity, due in part to control of the Cu₂O layer and elevated surface pH. Polymer-composite electrodes exhibit enhanced reactivity over a wide range of proton-involved electrochemical reactions. As an example, methanol oxidation reactivity is substantially enhanced with polymer-modified Pt electrodes.

9:40am SS1+HC-MoM-5 Enhancement of CO₂ Reduction Reaction Activity and Selectivity of Sub-2 nm Ag Electrocatalysts by Electronic Metal-Carbon Interactions, Xingyi Deng, D. Alfonso, T. Nguyen-Phan, D. Kauffman, National Energy Technology Laboratory

We show that the activity and selectivity of sub-2 nm Ag electrocatalysts for electrochemical CO₂ to CO conversion is drastically improved by electronic metal-support interactions (EMSI). The EMSIs between Ag and carbon support, created by deposition of Ag onto heavily sputtered, highly oriented pyrolytic graphite (HOPG), were revealed by X-ray photoelectron spectroscopy (XPS), and supported by computational modeling based on density functional theory (DFT). While sub-2 nm Ag electrocatalysts lack of EMSIs showed selectivity (CO Faradaic efficiency FE_{CO} < 2%) toward the electrochemical CO₂ reduction reaction (CO₂RR), similar sized Ag electrocatalysts with EMSIs demonstrated ~100% FE_{CO} and more than 15-fold increase of CO turnover frequency (TOF_{CO}). Our calculations elucidated that the electronic Ag-C interactions led to a significant charge transfer (1.02 e) from Ag to carbon support and subsequently lowered the potential-limiting step in CO₂RR by 0.41 eV. Our results provide the direct evidence of improving CO₂RR performances of electrocatalysts through EMSIs, particularly between metal and carbon. The EMSIs help break the limit of size-dependent CO₂RR activity in Ag nanoparticles, hinting at a new approach for creating active and selective electrocatalysts.

10:00am SS1+HC-MoM-6 Super Structure and Surface Reconstructions with High-Energy Surface X-Ray Diffraction, Gary Harlow, University of Oregon; D. Gajdek, University of Malmo, Sweden; G. Abbondanza, A. Grespi, Lund University, Sweden; H. Wallander, University of Malmo, Sweden; A. Larsson, University of Lund, Sweden; L. Merte, University of Malmo, Sweden; E. Lundgren, Lund University, Sweden

The performance of an electrocatalyst (its activity, selectivity, and stability) is strongly dependent on the electrode structure and composition, particularly in the near surface region. A successful approach in trying to understand the impact of structure is the use of well-defined model electrodes such as single crystals, to isolate how various changes in structure and composition impact upon the catalyst behavior. Surface x-ray diffraction gives the average surface structure of an isolated facet, whereas real catalysts often contain multiple facets and edge sites. This contribution will discuss the application of high energy surface x-ray scattering to quickly map out large volumes of 3D reciprocal space and then extract crystal truncation rods. These truncation rods can then be used to determine atomic coordinates of surface atoms, in operando.

Monday Morning, November 6, 2023

Examples during methanol oxidation on both Pt(111) and Au(111) surfaces will be presented. As well as measurements on the the stability of ultra-thin Fe oxide layers on Pt(111) after transfer from vacuum to our in situ electrochemical cell.

Laboratory-Based Ambient-Pressure X-ray Photoelectron Spectroscopy Focus Topic

Room B116 - Session LX+AS+BI+HC+SS+TH-MoA

Laboratory-Based AP-XPS:Surface Chemistry and Biological/Pharmaceutical Interfaces

Moderators: **Gregory Herman**, Argonne National Laboratory, **Ashley Head**, Brookhaven National Laboratory

1:40pm **LX+AS+BI+HC+SS+TH-MoA-1 The Role of Co-Adsorbed Water in Decomposition of Oxygenates**, *H. Nguyen, K. Chuckwu, Líney Árnadóttir*, Oregon State University **INVITED**

The decomposition of oxygenates in the presence of water finds various applications in chemical processes, such as biomass conversion. The presence of co-adsorbates and solvents affects both the reaction rate and selectivity. In this study, we used NAP-XPS and DFT to investigate the decomposition of acetic acid on Pd(111) as a model system for the decomposition of small oxygenates in the absence and presence of water. The decomposition of acetic acid occurs through two main reaction pathways, decarboxylation, and decarbonylation, forming CO₂ or CO, respectively. Our DFT calculations indicate that the two pathways have similar barriers without water. However, in the presence of water, the decarboxylation path becomes. Similarly, our AP-XPS experiments show an increase in the CO₂/CO ratio as well as a decrease in the CO/acetate-acetic acid and acetic acid/acetate ratios when water is present. The shift in selectivity is not due to a single reaction step, but rather the decreasing barrier in general for OH scissoring and the increasing barrier for C-O scissoring. This shift favors the formation of CO₂, as demonstrated by our microkinetic model.

2:20pm **LX+AS+BI+HC+SS+TH-MoA-3 Integrating First-principles Modeling and AP-XPS for Understanding Evolving Complex Surface Oxides in Materials for Hydrogen Production and Storage**, *B. Wood, Tuan Anh Pham*, Lawrence Livermore Laboratory **INVITED**

Chemical processes occurring at solid-gas, solid-liquid, and solid-solid interfaces critically determine the performance and durability of hydrogen production and storage technologies. While directly probing behavior of these interfaces under actual operating conditions remains challenging, modern surface science approaches such as ambient-pressure X-ray photoelectron spectroscopy (AP-XPS) can provide insight into the evolution of surface chemistry in approximate environments. However, interpretation of these spectra can be complicated: standards for complex surface chemical moieties are often unavailable, and bulk standards can be unreliable. First-principles computations are emerging as an important companion approach, offering the ability to directly compute spectroscopic fingerprints. This has the advantage of aiding interpretation of the experiments, while simultaneously using the experiment-theory comparison to inform construction of more accurate interface models. In this talk, I will show how computation has been combined with laboratory-based AP-XPS measurements to understand the evolving chemistry of complex native surface oxides. Two examples will be drawn from activities within the U.S. Department of Energy HydroGEN and HyMARC consortia, which focus on renewable hydrogen production and materials-based hydrogen storage, respectively. First, I will discuss the application to surface oxidation of III-V semiconductors for photoelectrochemical hydrogen production, which demonstrates transitions between kinetically and thermodynamically controlled oxidation regimes with implications for device performance. Second, I will also show how the same approach has been applied to understand the rate-determining role of surface oxides in the dehydrogenation performance of NaAlH₄ for solid-state hydrogen storage.

This work was performed under the auspices of the U.S. Department of Energy by Lawrence Livermore National Laboratory under Contract DE-AC52-07NA27344.

3:00pm **LX+AS+BI+HC+SS+TH-MoA-5 Particle Encapsulation on Reducible Oxides Under Near-Ambient Pressures**, *F. Kraushofer, M. Krinninger, P. Petzoldt, M. Eder, S. Kaiser, J. Planksky, T. Kratky, S. Günther, M. Tschurl, U. Heiz, F. Esch, Barbara A. J. Lechner*, TUM, Germany **INVITED**

Catalysts on reducible oxide supports often change their activity significantly at elevated temperatures due to the strong metal-support interaction (SMSI), which induces the formation of an encapsulation layer around the noble metal particles. However, the impact of oxidizing and

reducing treatments at elevated pressures on this encapsulation layer remains controversial, partly due to the 'pressure gap' between surface science studies and applied catalysis.

In the present work, we employ near-ambient pressure X-ray photoelectron spectroscopy (NAP-XPS) and scanning tunneling microscopy (NAP-STM) to study the effect of reducing and oxidizing atmospheres on the SMSI-state of well-defined oxide-supported Pt catalysts at pressures from UHV up to 1 mbar. On a TiO₂(110) support, we can either selectively oxidize the support or both the support and the Pt particles by tuning the O₂ pressure.^[1] We find that the growth of the encapsulating oxide overlayer is inhibited when Pt is in an oxidic state. Our experiments show that the Pt particles remain embedded in the support once encapsulation has occurred. On Fe₃O₄(001), the encapsulation stabilizes small Pt clusters against sintering.^[2] Moreover, the cluster size and thus footprint lead to a change in diffusivity and can therefore be used to tune the sintering mechanism. Very small clusters of up to 10 atoms even still diffuse intact after encapsulation.

[1] P. Petzoldt, P., M. Eder, S. Mackewicz, M. Blum, T. Kratky, S. Günther, M. Tschurl, U. Heiz, B.A.J. Lechner, Tuning Strong Metal-Support Interaction Kinetics on Pt-Loaded TiO₂ (110) by Choosing the Pressure: A Combined Ultrahigh Vacuum/Near-Ambient Pressure XPS Study, *J. Phys. Chem. C* 126, 16127-16139 (2022).

[2] S. Kaiser, J. Planksky, M. Krinninger, A. Shavorskiy, S. Zhu, U. Heiz, F. Esch, B.A.J. Lechner, Does Cluster Encapsulation Inhibit Sintering? Stabilization of Size-Selected Pt Clusters on Fe₃O₄(001) by SMSI, *ACS Catalysis* 13, 6203-6213 (2023).

4:00pm **LX+AS+BI+HC+SS+TH-MoA-8 Applications of NAP XPS in Pharmaceutical Manufacturing: Surface Analysis, Hydrogen Bonds, and Solute-Solvent Interactions**, *Sven Schroeder*, University of Leeds, UK **INVITED**

The availability of laboratory-based NAP XPS creates novel interface research opportunities for scientific disciplines and technology areas that deal with materials incompatible with traditional ultra-high vacuum XPS. This is, for example, the case for many organic and/or pharmaceutical materials and formulations, whose characterization by XPS has hitherto been restricted by their vapour pressures. NAP XPS permits for the first time systematic and detailed analysis of the light element photoemission lines (especially C/N/O 1s) in these materials. In conjunction with elemental analysis by survey XP spectra they provide quantitative information on composition and speciation both in the bulk and at the surfaces of pure organic solids, in their formulations with other components and in solutions. Especially of interest are studies of the solid/liquid interface with water, which is of high relevance for understanding and controlling drug release profiles from tablets. To illustrate these points I will present various examples of research on pharmaceutical materials. Moreover, near-ambient pressure core level spectroscopy turns out to be an extremely powerful probe for the structure and dynamics of hydrogen bonding and proton transfer in materials, both in the solid state and in solutions. NAP XPS measurements provide unique insight into proton dynamics in noncrystalline solids and liquids, where traditional characterisation by crystallography and nuclear magnetic resonance fails or provides ambiguous information on proton locations.

4:40pm **LX+AS+BI+HC+SS+TH-MoA-10 The Change of DNA and Protein Radiation Damage Upon Hydration: In-Situ Observations by Near-Ambient-Pressure XPS**, *Marc Benjamin Hahn*, Bundesanstalt für Materialforschung und -prüfung (BAM), Germany **INVITED**

X-ray photoelectron-spectroscopy (XPS) allows simultaneous irradiation and damage monitoring. Although water radiolysis is essential for radiation damage, all previous XPS studies were performed in vacuum. [1] Here we present near-ambient-pressure XPS experiments to directly measure DNA damage under water atmosphere. They permit in-situ monitoring of the effects of radicals on fully hydrated double-stranded DNA. Our results allow us to distinguish direct damage, by photons and secondary low-energy electrons (LEE), from damage by hydroxyl radicals or hydration induced modifications of damage pathways. The exposure of dry DNA to x-rays leads to strand-breaks at the sugar-phosphate backbone, while deoxyribose and nucleobases are less affected. In contrast, a strong increase of DNA damage is observed in water, where OH-radicals are produced. In consequence, base damage and base release become predominant, even though the number of strand-breaks increases further. Furthermore, first data about the degradation of single-stranded DNA binding-proteins (GSP / GV5 and hmtSSB) under vacuum and NAP-XPS conditions are presented.

Monday Afternoon, November 6, 2023

[1] Hahn, M.B., Dietrich, P.M. & Radnik, J. In situ monitoring of the influence of water on DNA radiation damage by near-ambient pressure X-ray photoelectron spectroscopy. *Commun Chem* 4, 50, 1-8 (2021). <https://doi.org/10.1038/s42004-021-00487-1>

Surface Science Division

Room D136 - Session SS+2D+AS+HC-TuM

Oxide and Chalcogenide Surfaces and Interfaces

Moderators: Rachael Farber, University of Kansas, Gareth Parkinson, TU Wien

8:00am **SS+2D+AS+HC-TuM-1 ViPerLEED: LEED-I(V) Made Easy, Alexander Michael Imre¹**, TU Wien, Austria; *F. Kraushofer*, TU Munich, Germany; *T. Kijlsinger, L. Hammer*, Friedrich-Alexander-University Erlangen-Nürnberg (FAU), Germany; *M. Schmid, U. Diebold, M. Riva*, TU Wien, Austria

Most surface science laboratories are equipped with a low-energy electron diffraction (LEED) setup. LEED patterns provide quick, qualitative insight into surface structure and ordering. However, the diffracted electron beams contain a large amount of additional structural information which is often ignored. By studying the diffraction intensities as a function of incident electron energy [LEED-I(V)], it is possible to quantitatively compare experimentally observed surfaces with structural models.

Despite the clear need for such a direct experiment-to-theory comparison, LEED-I(V) is only routinely used by few specialized groups. A main obstacle for widespread adoption is that existing solutions for LEED-I(V) analysis and simulation are time-consuming and hard to use for scientists who are not already experts in the field.

To resolve this issue, we have developed the Vienna Package for Erlangen LEED (ViPerLEED) – a package of three independent but complementary tools for easy LEED-I(V) acquisition and analysis. All parts of ViPerLEED will be released as open source at the time of publishing:

1. **Electronics:** We provide schematics and control software for electronics, which allows users to easily and cheaply upgrade most existing LEED setups for acquiring high-quality LEED-I(V) data. These ViPerLEED electronics are based on an Arduino microcontroller and can be home-built from off-the-shelf components. The associated control software synchronizes with the camera and automates the experiment.
2. **Spot-tracker:** ViPerLEED provides a plugin for the public-domain image processing program ImageJ, for spot tracking and extraction of LEED-I(V) spectra from series of raw diffraction images. The automatically extracted I(V) curves can be used for further analysis or as a fingerprint of the surface surface. The plugin package also provides user-friendly options for examination, selection and smoothing of the I(V) data.
3. **Simulation software:** For structure analysis, we introduce a Python package for calculation of LEED-I(V) spectra and structure optimization. This software is based on the established TensErLEED package and extends its functionality while still making it easy for new users to get started with the technique. It uses standard file formats for the surface structure, provides automated symmetry detection, and requires just a handful of parameters for running a structure determination.

8:20am **SS+2D+AS+HC-TuM-2 Quasicrystal-like Ordering of the La_{0.8}Sr_{0.2}MnO₃(001) Surface, Erik Rheinfrank, G. Franceschi, L. Lezuo, M. Schmid, U. Diebold, M. Riva**, TU Wien, Austria

Lanthanum-strontium manganite (La_{0.8}Sr_{0.2}MnO₃, LSMO) is a perovskite oxide used as a cathode material in solid oxide fuel cells, which convert chemical energy to electrical energy. To gain deeper insights into the reaction mechanisms, it is important to understand the structure of the surface at the atomic scale. To this end, we grow atomically flat single-crystalline LSMO thin films on Nb-doped SrTiO₃ (STO) substrates via pulsed laser deposition (PLD). Previously, this has been achieved for the (110) orientation.^[1,2] Here, we use a similar approach on the (001) surface that is commonly used for oxide-based electronics and spintronics. The as-grown films have a MnO_x terminated surface that shows a 4-fold symmetric structure in low-energy electron diffraction (LEED), best explained by a set of four basis vectors reminiscent of quasicrystals. Scanning tunnelling microscopy (STM) and Q+ non-contact atomic force microscopy (nc-AFM) reveal an aperiodic arrangement of tiles with rotation angles of $\pm 26.6^\circ$ and $90 \pm 26.6^\circ$, and a Fourier transform consistent with the LEED pattern. As for

quasicrystals, the surface has a sharp diffraction pattern despite the lack of translational symmetry.

[1] Franceschi *et al.*, J. Mater. Chem. A, 2020, **8**, 22947-22961

[2] Franceschi *et al.*, Phys. Rev. Materials, 2021, **5**, L092401

8:40am **SS+2D+AS+HC-TuM-3 AVS Graduate Research Awardee Talk: The Selective Blocking of Potentially Catalytically-Active Sites on Surface-Supported Iron Oxide Catalysts, Dairong Liu^{2,3}, N. Jiang**, University of Illinois - Chicago

The extensive research on ultrathin ferrous oxide (FeO) islands and films over the last few decades has significantly contributed to the understanding of their structural and catalytic properties. One important aspect that has been investigated is the surface properties of ultrathin FeO islands, particularly the role played by the edges of these islands in catalytic reactions, such as CO oxidation. So far, two different types of edge, Fe-terminated edge and O-terminated edge, have been identified in the well-growth FeO island. However, despite this significant progress, the local chemical properties of these two types of edges, including their metal affinity, have remained largely unexplored. Here, we used scanning tunneling microscopy (STM) to study the interaction of Pd and Pt with FeO grown on Au(111). Different Fe affinities for Pd and Pt are demonstrated by the preferential growth of Pd on the Fe-terminated edge and Pt on the O-terminated edge of FeO nanoislands, resulting in selectively blocked FeO edges. In addition to revealing the different metal affinities of FeO edges, our results provide new insights into the edge reactivity of FeO/Au(111) and suggest an approach for controlling the selectivity of FeO catalysts. By comparing the behavior of different edges in the catalysis reaction, the catalytic activity of these edges can be studied solely, thereby sheds light into the future modification of ferrous-based catalysts.

9:00am **SS+2D+AS+HC-TuM-4 Unraveling Surface Structures of Ga-Promoted Transition Metal Catalysts in CO₂ Hydrogenation, Si Woo Lee, S. Shaikhutdinov, B. Roldan Cuenya**, Fritz Haber Institute of the Max Planck Society, Germany

Gallium-containing alloys with transition metals (TM) have recently been reported to be reactive in the selective hydrogenation of CO₂ for methanol synthesis. However, a full understanding of the Ga-promoted catalysts is still missing due to the lack of information about the *surface* structures formed under reaction conditions. In this respect, studies using surface-sensitive techniques applied to well-defined model systems can provide key information to elucidate the reaction mechanism and provide the basis for the rational design of Ga-promoted catalysts.

In this work, we employed *in-situ* Near Ambient Pressure Scanning Tunneling Microscopy (NAP-STM) and X-ray Photoelectron Spectroscopy (NAP-XPS), which make it possible to study surfaces in the reaction conditions, for monitoring the structural and chemical evolution of the Ga-covered Cu surfaces in the CO₂ hydrogenation reaction. NAP-STM images recorded in the reaction mixture revealed temperature- and pressure-dependent de-alloying of the initially formed, well-ordered ($\sqrt{3} \times \sqrt{3}$)R30°-Cu(111) surface alloy and the formation of Ga-oxide islands embedded into the Cu(111) surface, exposing GaO_x/Cu(111) interfacial sites. Notably, in our atomically-resolved STM image of Ga-oxide/Cu(111), it is clearly observed that Ga-oxide grows into an ultrathin oxide layer form with (4 $\sqrt{3} \times 4\sqrt{3}$)R30° superstructure. From NAP-XPS studies on Ga/Cu(111) in the presence of CO₂ and H₂, the formation of formate was observed, and this reaction intermediate was eventually transformed into methoxy at elevated temperatures, representing the final surface-bound intermediate for methanol synthesis. In contrast to Ga-containing Cu catalyst, on the other hand, there was no reaction intermediate at high temperature on the Ga-free Cu(111) surface, demonstrating that further reactions do not occur anymore from chemisorbed CO₂^{δ-} on Cu surface alone. Therefore, the GaO_x/Cu interface formed under reaction conditions may expose catalytically active sites never considered for this reaction before. We believe that our experimental results shed light on the complex surface structure of Ga-containing catalytic systems, which is only possible to obtain using state-of-the-art experimental techniques under reaction conditions. Only by establishing the atomic structure of the Ga-oxide layer(s) and its interface to the transition metal under working conditions can one bring insight into the reaction mechanism of this methanol synthesis catalyst.

¹ SSD Morton S. Traum Award Finalist

² AVS Graduate Research Awardee

³ SSD Morton S. Traum Award Finalist

Tuesday Morning, November 7, 2023

9:20am **SS+2D+AS+HC-TuM-5 Ultrathin Metal Oxide, Nitride and Sulfide Films: Bringing the Well-Known Compounds to a Unit-Cell Thickness**, **Mikolaj Lewandowski**, NanoBioMedical Centre, Adam Mickiewicz University in Poznań, Poland **INVITED**

Bringing the well-known materials from bulk size to a unit-cell thickness may significantly influence their structure and physicochemical properties. As an example, ultrathin (< 1-nanometer-thick) films of metal/non-metal compounds, such as metal oxides, nitrides or sulfides epitaxially grown on single-crystal supports, are characterized by unique electronic, catalytic and magnetic properties not observed for their bulk counterparts. Such films also exhibit superior structural flexibility, undergoing phase transitions upon exposure to external factors (such as reactive gases or high temperatures) [1,2]. All this makes them promising candidates for applications in various technological fields, including nanoelectronics, spintronics and heterogeneous catalysis.

Within the lecture, I will address the growth, structure and properties of ultrathin metal oxide, nitride and sulfide films, with compounds of iron as exemplary cases. The scanning tunneling microscopy and spectroscopy (STM/STS), low energy electron diffraction (LEED), X-ray photoelectron spectroscopy (XPS), low energy electron microscopy (LEEM) and density functional theory (DFT) results – obtained by my group and our collaborators – provide universal guidelines for designing ultrathin films with desired structure and properties [1–3].

[1] Y. Wang, G. Carraro, H. Dawczak-Dębicki, K. Synoradzki, L. Savio, M. Lewandowski, *Applied Surface Science* 528 (2020) 146032.

[2] N. Michalak, T. Ossowski, Z. Miłosz, M. J. Prieto, Y. Wang, M. Werwiński, V. Babacic, F. Genuzio, L. Vattuone, A. Kiejna, Th. Schmidt, M. Lewandowski, *Advanced Materials Interfaces* 9 (2022) 2200222.

[3] P. Wojciechowski, W. Andrzejewska, M.V. Dobrotvorska, Y. Wang, Z. Miłosz, T. Ossowski, M. Lewandowski, submitted (2023).

The author acknowledges financial support from the National Science Centre of Poland (through SONATA 3 2012/05/D/ST3/02855, PRELUDIUM 11 2016/21/N/ST4/00302 and M-ERA.NET 2 2020/02/Y/ST5/00086 projects), as well as the Foundation for Polish Science (First TEAM/2016-2/14 (POIR.04.04.00-00-28CE/16-00) project co-financed by the European Union under the European Regional Development Fund).

11:00am **SS+2D+AS+HC-TuM-10 Optimized Infrared Reflection Absorption Spectroscopy for Metal Oxides: Overcoming Challenges of Low Reflectivity and Sub-Monolayer Coverage**, **Jiri Pavelec**, **D. Rath**, **M. Schmid**, **U. Diebold**, **G. Parkinson**, Vienna University of Technology, Austria

Infrared reflection absorption spectroscopy (IRAS) is a wide-spread technique in heterogeneous catalysis, and it is an ideal tool for the comparison of real and model catalysts [1]. Most surface science groups perform IRAS studies either directly on metal single crystals, or on (ultra-)thin metal oxide films grown on such samples [2]. Achieving high-quality data from metal-oxide single crystal surfaces is difficult because their low reflectivity necessitates averaging many individual measurements with long acquisition times [3]. The goal of this work was to develop an IRAS setup for studying the adsorption of molecules on model “single-atom” catalysts. Here, the low reflectivity of oxide support is exacerbated by the sub-monolayer coverage of adsorbates on single adatoms. In the contribution, I will present the novel IRAS system we have developed to overcome these two challenges.

The main improvements over commonly-used setups are a high numerical aperture, an optimized optical path, control of the incidence angle range, and high mechanical stability. The high numerical aperture of the optical system leads to an increase in the amount of light reflected from a small single crystal sample. This is achieved by placing both the illumination and collector mirrors inside the UHV chamber close to the sample. To minimize the loss of signal, optimization of the optical path was performed using a ray tracing program. The other limit is the small area on the sample that is covered with adsorbates: in our setup, a molecular beam delivers adsorbates with a spot diameter of 3.5 mm [4]. Infrared light is reflected only from this area.

The reflectivity and absorbance of non-metallic samples varies strongly with incidence angle, and can even change a sign, leading to cancellation. The optimum angle ranges are different for every material. As our setup has a large range of incident angles, we can use this to our advantage: Using two adjustable aperture plates, we can vary the minimum and maximum incidence angle from 49° to 85° to maximize the signal for each single crystal sample. Angle control also allows us to optimize the signal for both p-polarized and s-polarized light independently.

We successfully executed and compared D₂O and CO absorbance measurements on a rutile TiO₂(110) surface, and our results agree with the established literature [3]. By properly selecting the incidence angle range, we achieved a signal-to-noise ratio of ~16 for 1 ML CO adsorbed on TiO₂ with only 150 seconds of measurement time.

[1] F. Zaera, *Chem. Soc. Rev.*, 43, 2014

[2] J. Libuda et al., *J. Chem. Phys.*, 114, 10, 2001

[3] N. G. Petrik et al., *The Journal of Physical Chemistry C*, 126 (51), 2022

[4] J. Pavelec et al., *J. Chem. Phys.*, 146, 2017

11:20am **SS+2D+AS+HC-TuM-11 VO Cluster-Stabilized H₂O Adsorption on a TiO₂ (110) Surface at Room Temperature**, **Xiao Tong**, Brookhaven National Laboratory

We probe the adsorption of molecular H₂O on a TiO₂ (110)-(1 × 1) surface decorated with isolated VO clusters using ultrahigh-vacuum scanning tunneling microscopy (UHV-STM) and temperature-programmed desorption (TPD). Our STM images show that preadsorbed VO clusters on the TiO₂ (110)-(1 × 1) surface induce the adsorption of H₂O molecules at room temperature (RT). The adsorbed H₂O molecules form strings of beads of H₂O dimers bound to the 5-fold coordinated Ti atom (5c-Ti) rows and are anchored by VO. This RT adsorption is completely reversible and is unique to the VO-decorated TiO₂ surface. TPD spectra reveal two new desorption states for VO stabilized H₂O at 395 and 445 K, which is in sharp contrast to the desorption of water due to recombination of hydroxyl groups at 490 K from clean TiO₂(110)-(1 × 1) surfaces. Density functional theory (DFT) calculations show that the binding energy of molecular H₂O to the VO clusters on the TiO₂ (110)-(1 × 1) surface is higher than binding to the bare surface by 0.42 eV, and the resulting H₂O-VO-TiO₂ (110) complex provides the anchor point for adsorption of the string of beads of H₂O dimers.

11:40am **SS+2D+AS+HC-TuM-12 Synthesis and Multimodal Characterization of Thin-Film Oxides**, **Dario Stacchiola**, Brookhaven National Laboratory

Thin films of metal oxides exhibit a variety of unique physical and chemical properties leading to broad applications in optics, microelectronics, optoelectronics, superconducting circuits, gas sensors, thermal catalysis, electrocatalysis, and solar energy harvesting. Many metal oxides can form stoichiometric and non-stoichiometric alloys and compounds with each other, commonly known as complex metal oxides. Alloy and compound formation, including growth and process conditions, offer great flexibility for manipulating the lattice, atomic scale structure motifs, and electronic structure to realize desired properties. In order to exploit this potential, knowledge about fundamental processes and atomic level structural information is required. We present here the synthesis and multimodal characterization of mixed-oxide films based on silica and titania, from single layers to complex metal oxides.

1. “Deciphering phase evolution in complex metal oxide thin films via high-throughput materials synthesis and characterization”, *Nanotechnology* 34, 125701 (2023)

2. “Resolving the evolution of atomic layer deposited thin film growth by continuous in situ X-ray absorption spectroscopy”, *Chem. Mat.* 33, 1740-1751 (2021)

3. “First-Principles Study of Interface Structures and Charge Rearrangement at the Aluminosilicate / Ru(0001) Heterojunction” *J. Phys. Chem. C* 123, 7731–7739 (2019)

12:00pm **SS+2D+AS+HC-TuM-13 Atomic Structure of Reconstructed Al₂O₃(0001) Surface**, **J. Hütner**, **A. Conti**, TU Wien, Austria; **D. Kugler**, CEITEC, Czechia; **F. Mittendorfer**, **U. Diebold**, **M. Schmid**, **Jan Balajka**, TU Wien, Austria

Corundum α-Al₂O₃ is an important ceramic widely used in electronics, optical applications, or as catalyst support. Despite its importance, the atomic structure of the most stable (0001) termination has not been conclusively determined. Detailed studies of Al₂O₃ surfaces have been stymied by its insulating nature, preventing the use of many surface science methods.

Structural models based on surface X-ray diffraction (SXRD) [1], and atomic force microscopy (AFM) [2], concluded the (√31 × √31)R±9°-reconstructed Al₂O₃(0001) surface formed upon high-temperature annealing is terminated by one or two layers of metallic Al strained to lattice-match the oxide substrate.

We imaged the reconstructed Al₂O₃(0001) surface with noncontact AFM (nc-AFM) using specifically functionalized tips for chemically-sensitive

Tuesday Morning, November 7, 2023

contrast. In particular, CuO_x terminated tips [3], enabled us to directly identify oxygen and aluminum atoms in the topmost layer.

With the aid of *ab-initio* calculations, we propose a structural model of the $(\sqrt{31} \times \sqrt{31})R\pm 9^\circ$ -reconstructed $\text{Al}_2\text{O}_3(0001)$ surface consistent with atomically resolved nc-AFM images and area-averaging spectroscopic data. Unlike prior models, the surface does not contain a metallic Al layer but consists of oxygen and aluminum atoms arranged in similar structural units as reported in thin AlO_x films [4,5].

[1] G. Renaud, et al., *Phys. Rev. Lett.* **73**, 13 (1994)

[2] J. V. Lauritsen, et al., *Phys. Rev. Lett.* **103**, 076103 (2009)

[3] B. Shulze Lammers, et al., *Nanoscale* **13**, 13617 (2021)

[4] G. Kresse, et al., *Science* **308**, 1440 (2005)

[5] M. Schmid, et al., *Phys. Rev. Lett.* **99**, 196104 (2007)

Surface Science Division

Room D136 - Session SS+HC-TuA

Photochemistry

Moderators: Erik Jensen, University of Northern British Columbia, Ahmad Nawaz, Hebrew University of Jerusalem

2:20pm SS+HC-TuA-1 Pt Nanoclusters on GaN Nanowires for Solar-Assisted Seawater Hydrogen Evolution, Victor Batista, W. Dong, Y. Xiao, K. Yang, Z. Ye, P. Zhou, I. Navid, Z. Mi, Yale University **INVITED**

Seawater electrolysis provides a viable method to produce clean hydrogen fuel. To date, however, the realization of high-performance photocathodes for seawater hydrogen evolution reaction has remained challenging. Here, we introduce n+p Si photocathodes with dramatically improved activity and stability for hydrogen evolution reaction in seawater, modified by Pt nanoclusters anchored on GaN nanowires (Fig 1). We find that Pt-Ga sites at the Pt/ GaN interface promote the dissociation of water molecules and spilling H* over to neighboring Pt atoms for efficient H₂ production. Pt/GaN/Si photocathodes achieve a current density of ~10 mA/cm² at 0.15 and 0.39 V vs. RHE and high applied bias photon-to-current efficiency of 1.7% and 7.9% in seawater (pH = 8.2) and phosphate-buffered seawater (pH = 7.4), respectively. We further demonstrate a record-high photocurrent density of ~169 mA/cm² under concentrated solar light (9 suns). Moreover, Pt/GaN/Si can continuously produce H₂ even under dark conditions by simply switching the electrical contact. This work provides valuable guidelines to design an efficient, stable, and energy- saving electrode for H₂ generation by seawater splitting.

3:00pm SS+HC-TuA-3 Photoreactivity of Single Micro-Sized TiO₂ Crystals, H. Zhu, W. Lu, K. Park, Zhenrong Zhang, Baylor University

Understanding the reactivity of TiO₂ particles with different polymorphs and morphologies is important for many photocatalytic applications. Here, the reactivity of individual anatase TiO₂ microcrystals with a large percentage of (001) facet was monitored and studied using operando photoluminescence microscopy. The photoreduction of resazurin on anatase microcrystals shows that the photoreduction rate on each microcrystal was different although the microcrystals had comparable sizes and exposed the same facets. The reaction rate changes from no reactivity to higher than that of the anatase (001) bulk single crystal. The reaction rate of the anatase microcrystals depends on the morphology and the structure of each particle. The reactivities of the microcrystals with mixed anatase-rutile phases and after the anatase-to-rutile phase transformation have also been monitored.

3:20pm SS+HC-TuA-4 Electron Induced Photochemistry of Nitrous Oxide-Water Co-Adsorbed Film (N₂O@H₂O) as a Model Study of Astrochemistry in the Interstellar Medium, Ahmad Nawaz, The Hebrew University of Jerusalem, Israel

The desorption kinetics of N₂O@H₂O film deposited on a Ru (0001) surface under ultra-high vacuum (UHV) environment (2x10⁻¹⁰ Torr) has been investigated as a model study for electrons-induced reactivity that takes place in the interstellar medium, using temperature-programmed desorption (TPD) measurements, at substrate temperature of 35K. The TPD spectra of all the prominent product masses were well detected by the QMS, employing a 3D-TPD analysis. The N₂O molecules, embedded within ASW as the host matrix, decompose upon exposure to electrons at kinetic energies of 10eV and 50 eV. This leads to the formation of new molecular products at m/z values of 28 (N₂) and 30 (NO) as the primary products. Typical TPD spectra of the parent N₂O molecules, while embedded in ASW layer (15 ML) are shown in Figure 1a and product formation is shown in Figure 1b. Here, the primary N₂O TPD peaks appear at ~82K, while some of these molecules are trapped within the water film and desorb together with the main ASW film at ~160K.

4:20pm SS+HC-TuA-7 Structure and Chemistry of Aqueous Oxide Interfaces from Molecular Simulations, A. Selloni, A. Raman, Princeton University; Marcos Calegari Andrade, Lawrence Livermore National Laboratory; B. Wen, Henan University, China **INVITED**

Photo-electrocatalysis involving complex oxide-water interfaces is a highly promising technology for the sustainable production of fuels. However, probing these complex interfaces and gaining atomistic insights is still very challenging for current experimental methods, and is often only possible through accurate computational simulations. In this talk I will discuss some of our recent work on the application of ab-initio based molecular

simulations to understand the structure and dynamics of interfacial water on photoelectrochemically relevant oxide surfaces. Specific topics will include proton transfer at the aqueous TiO₂ and IrO₂ interfaces and the influence of surface atomic structure on the water dissociation fraction and hydroxyl lifetimes at the interface.

5:00pm SS+HC-TuA-9 Photodissociation of an Adsorbate via Coadsorbate Photon Absorption: Electronic Energy Transfer in Heterogeneous Molecular Thin Films, Erik Jensen, University of Northern B.C., Canada

The photophysics of many small aromatics and related molecular systems has been studied intensely and widely for many years, both in understanding the molecular origins of natural phenomenon such as photosynthesis, as well as in areas of technological interest. Although the UV photosensitization of CH₃I dissociation in gas-phase mixtures with benzene was noted many years ago[1], we can find no subsequent examples of studies of the photochemical dynamics of this process. We have studied a set of thin film molecular systems on a metal substrate using UHV surface science techniques and time-of-flight spectroscopy on neutral photofragments.

In the present work, we have studied the dynamics of the near-UV photodissociation of CH₃I adsorbed on thin films (1–10ML) of benzene[2] and a variety of fluorinated benzenes grown on a Cu(100) substrate. Using polarized 248nm light, we find that the kinetic energies of the CH₃ photofragments point to significantly altered CH₃I dissociation dynamics when adsorbed on C₆H₆, C₆H₅F and C₆H₄F₂ thin films, with progressive changes in the observed dynamics as higher fluorobenzenes are used (up to C₆F₆). The altered CH₃I photodissociation dynamics and coincidentally increased effective photodissociation cross sections are ascribed to a new pathway with initial photoabsorption in the aromatic thin film, and the excitation energy being efficiently transported to the CH₃I adsorbed on top. There is evidence that excitons in the aromatic thin film play a significant role in the transport and transfer of the electronic excitation to the CH₃I top layer.

References

- [1] Dubois, J.T. and Noyes Jr., W.A., *Photochemical Studies XLVI: Photosensitization by Benzene and Pyridine Vapours*, J. Chem. Phys. **19**, 1512 (1951).
- [2] Jensen, E.T., *Contrasting Mechanisms for Photodissociation of Methyl Halides Adsorbed on Thin Films of C₆H₆ and C₆F₆*. Phys. Chem. Chem. Phys. **23**, 3748 (2021).

5:20pm SS+HC-TuA-10 UV-Induced Oxidation of Aluminum, Robert Berg, C. Tarrío, T. Lucatorto, National Institute of Standards and Technology (NIST); F. Eparvier, A. Jones, Laboratory for Atmospheric and Space Physics

Aluminum oxide films are usually grown on aluminum metal by anodization in a liquid electrolyte (thick films) or heating in the presence of oxygen gas (thin films). A third way is to expose the aluminum to ultraviolet radiation (UV) in the presence of water vapor. We devised a model of such oxidation that combined descriptions of photoemission from the Al metal, electron-phonon scattering in the oxide, Al³⁺ ion transport in the oxide, and the adsorption and ionization of H₂O on the oxide surface. It also accounted for UV-induced desorption of H₂O and the effect of the Al³⁺ ion flux on the surface reactions.

The model's five free parameters were fit to our measurements of UV-induced oxidation of aluminum. The UV, which was produced by filtering synchrotron radiation, comprised wavelengths from 150 nm to 480 nm, and the H₂O pressure was varied between 3 × 10⁻⁸ mbar and 1 × 10⁻⁴ mbar. Exposures lasted from 3 hours to 20 days. An exposure with oxygen instead of water caused oxidation consistent with the background H₂O pressure; the oxygen caused no additional oxidation.

The parameter values fitted to our measurements allowed us to describe the oxidation of aluminum membranes that were used to filter extreme UV wavelengths on the Solar Dynamics Observatory, a sun-observing satellite. This new understanding will help prevent similar problems on future satellites. These results are the first experimental confirmation of a model of UV-induced oxidation.

Tuesday Afternoon, November 7, 2023

5:40pm **SS+HC-TuA-11 Self-Induced and Progressive Photo-Oxidation of Organophosphonic Acid Grafted Titanium Dioxide**, *Nick Gys*, Vrije Universiteit Brussel, Belgium; *B. Pawlak*, Hasselt University, Belgium; *K. Marcoen*, Vrije Universiteit Brussel, Belgium; *G. Reekmans*, Hasselt University, Belgium; *L. Fernandez Velasco*, Royal Military Academy, Belgium; *R. An*, University of Antwerp, Belgium; *K. Wyns*, Flemish Institute for Technological Research, Belgium; *K. Baert*, Vrije Universiteit Brussel, Belgium; *K. Zhang*, *L. Lufungula*, University of Antwerp, Belgium; *A. Piras*, Hasselt University, Namur University, Belgium; *L. Siemons*, University of Antwerp, Belgium; *B. Michielsen*, Flemish Institute for Technological Research, Belgium; *S. Van Doorslaer*, *F. Blockhuys*, University of Antwerp, Belgium; *T. Hauffman*, Vrije Universiteit Brussel, Belgium; *P. Adriaensens*, Hasselt University, Belgium; *S. Mullens*, Flemish Institute for Technological Research, Belgium; *V. Meynen*, University of Antwerp, Belgium

The introduction of organic molecules onto the surface of metal oxides through surface grafting provides the ability to tailor the surface properties towards an increased specificity and control of interactions. In the field of hybrid organic-inorganic materials, organophosphonic acid (PA) grafted metal oxides are becoming increasingly more prominent given their versatility in surface tuning and their specific merits in applications ranging from supported metal catalysis⁽¹⁾, hybrid (photo)-electric devices⁽²⁾, biosensing⁽³⁾ and sorption and separation processes.⁽⁴⁾ While synthesis-properties-performance correlations are being studied for organophosphonic acid grafted TiO₂, their stability and the impact of exposure conditions on possible changes in the interfacial surface chemistry remain unexplored. In addition, a differentiation in the stability of the organic group (carbon chain) and the M-O-P bonds is missing. In this study⁽⁵⁾, the impact of different ageing conditions on the evolution of the surface properties of propyl- and 3-aminopropylphosphonic acid grafted mesoporous TiO₂ over a period of 2 years is reported, using solid-state ³¹P and ¹³C NMR, ToF-SIMS, EPR and XPS as main techniques. In humid conditions under ambient light exposure, PA grafted TiO₂ surfaces initiate and facilitate photo-induced oxidative reactions, resulting in the formation of phosphate species and degradation of the grafted organic group with a loss of carbon content ranging from 40 to 60 wt%. Since exposure under dry air does not result in ageing phenomena, humidity and more specifically, the interactions of adsorbed water with the grafted surface, play a fundamental role in the ageing process. By revealing the underlying ageing mechanism, solutions were provided to prevent degradation. This work creates critical awareness in the research community working on hybrid titania materials and other possible photo-active materials to evaluate changes in photo-activity and stability after surface grafting.

1. F. Forato et al., Chem. - A Eur. J. 24, 2457–2465 (2018).
2. H. Chen, W. Zhang, M. Li, G. He, X. Guo, Chem. Rev. 120, 2879–2949 (2020).
3. N. Riboni et al., RSC Adv. 11, 11256–11265 (2021).
4. G. A. Seisenbaeva et al., RSC Adv. 5, 24575–24585 (2015).
5. N. Gys et al., Chempluschem. 88 (2023), doi:10.1002/cplu.202200441.

6:00pm **SS+HC-TuA-12 "Laser-XPS" invented 1989 in Japan, Patented 1997**, *B. Vincent Crist*, XPS Library

In 1989, a novel technique, Laser-XPS, was developed. Laser-XPS uses XPS to probe the core level surface chemical physics of various solid state materials while the materials are held in an ultra-high vacuum (UHV) chamber and irradiated with CW tunable organic dye or argon ion lasers. These two tunable CW lasers provide energy in the 1.9-3.5 eV range (655-351 nm, 44-81 Kcal/mol) with power levels ranging from 100-1,000 mW. A dynamic mode of operation uses XPS to directly measure the electronic nature of the photo-excited states, the photo-thermal effects, and the lifetimes of the associated initial and final states produced by the tunable CW laser irradiation. Several reversible phenomena, which are wavelength or power level dependent, were observed via the dynamic mode. These phenomena include: energy shifts in XPS signals, changes in XPS peak widths, charge control quality, and phosphorescence during XPS. A sequential mode of operation makes it possible to study the non-reversible effects of irradiating materials under UHV conditions with CW lasers. Non-reversible phenomena observed via the sequential mode include: surface chemical reactions, elimination of adventitious carbon contamination, elimination of oxygen species associated with the presence of water, hydroxides, or carbonates, color changes, outgassing, and melting. The initially expected energy shifting of a specific XPS signal within a complex spectrum of XPS signals from very similar chemical species due to narrow, selective photo-excitation of specific valence bands, was, however, not realized in this preliminary study.

Fundamental Discoveries in Heterogeneous Catalysis Focus Topic

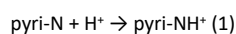
Room B113 - Session HC+SS-WeM

Origins of Single Atom Catalysis

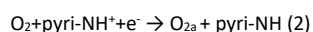
Moderators: Rachael Farber, University of Kansas, Gareth Parkinson, TU Wien

8:00am **HC+SS-WeM-1 Role of Pyridinic Nitrogen in the Mechanism of the Oxygen Reduction Reaction on Carbon Electrocatalysts**, *Kotaro Takeyasu*, University of Tsukuba, Japan; *S. Singh*, Shiv Nadar University, India; *K. Homma*, *K. Hayashida*, University of Tsukuba, Japan; *S. Ito*, *T. Morinaga*, National Institute of Technology, Tsuruoka College, Japan; *Y. Endo*, *M. Furukawa*, University of Tsukuba, Japan; *T. Mori*, National Institute for Materials Sciences (NIMS), Japan; *H. Ogasawara*, SLAC National Laboratory; *J. Nakamura*, International Institute for Carbon-Neutral Energy Research, Kyushu University, Japan

Nitrogen doped carbon catalysts are promising Pt-free catalysts for the oxygen reduction reaction (ORR) in polymer electrolyte fuel cells owing to the high durability and the high activity in alkaline media. The primary active site in N-doped carbon catalysts is the pyridinic nitrogen (pyri-N), which is bound to two carbon atoms with negative charge.[1] However, a large barrier of N-doped carbon catalysts for the commercial usage is the decreased activity in acidic media. Hence, we investigated this deactivation phenomenon to widen the applicability of N-doped carbon catalysts. In acidic media, the protonation of pyri-N (pyri-NH⁺) occurs as the first step owing to the basicity of pyri-N.



As the following process, we have demonstrated the electrochemical reduction of pyri-NH⁺ coupled with thermal O₂ adsorption on carbon atoms near pyri-NH⁺ using model catalysts:



In this reaction, the thermal adsorption of O₂ let the electrochemical reduction of pyri-NH⁺ to pyri-NH thermodynamically favorable due to the adsorption energy of O₂. Although the formation of pyri-NH⁺ is a cause of the decrease in ORR activity, but pyri-NH⁺ itself is essential for the formation of pyri-NH and the adsorption of O₂. A key point is that a dope electron into π* orbital of π-conjugative system near pyri-NH promotes the adsorption of O₂. However, the hydration of pyri-NH⁺ forming pyri-NH⁺ · (H₂O)_n causes a lower shift in the redox potential and consequently, Eq. 2 becomes the rate-determining step (RDS). Therefore, we consider that the hydration of pyri-NH⁺ is the main cause of the decrease in ORR activity in acid electrolytes.[2] Thus, we hypothesize an enhanced ORR activity by the introduction of hydrophobicity in the vicinity of pyri-NH⁺, suppressing the extent of hydration.

Introducing the hydrophobic cavity prevented the hydration of pyri-NH⁺ but inhibited the proton transport. We then increased proton conductivity in the hydrophobic cavity by introducing SiO₂ particles coated with ionic liquid polymer/Nafion® which kept the high onset potentials with an increased current density even in acidic media.[3]

References

- [1] D. Guo, J. Nakamura et al., *Science*, 2016, 351, 361-365.
- [2] K. Takeyasu, J. Nakamura et al., *Angew. Chem. Int. Ed.* 60, 5121 (2021).

[3] S. K. Singh, K. Takeyasu, J. Nakamura et al., *Angew. Chem. Int. Ed.* 61, e202212506 (2022).

8:20am **HC+SS-WeM-2 Atomic-Level Studies of Mono-Carbonly and Gem-Dicarbonyl Formation on Rh-Decorated Fe₃O₄(001)**, *Panukorn Sombut*, *C. Wang*, *L. Puntscher*, *M. Meier*, *J. Pavelec*, *Z. Jakub*, *M. Schmid*, *U. Diebold*, TU Wien, Austria; *C. Franchini*, University of Vienna, Austria; *G. Parkinson*, TU Wien, Austria

Understanding the interaction between reactant molecules and “single atom” active sites is important for comprehending the evolution of single-atom catalysts in reactive atmospheres. Here, we study how Fe₃O₄(001)-supported¹ Rh₁ monomers and Rh₂ dimer species interact with CO using density functional theory (DFT), combined with temperature-programmed desorption, x-ray photoelectron spectroscopy, and in-situ scanning tunneling microscopy techniques. Our results show that stable Rh₁(CO)₁ monocarbonyls are the exclusive product of CO adsorption at both 2-fold and 5-fold coordinated Rh₁ sites, but the different coordination environment leads to different adsorption energies. The DFT calculations reveal that the Rh₁(CO)₁ formed at the 5-fold coordinated Rh₁ site adopts an octahedral structure, while the Rh₁(CO)₁ formed at the 2-fold coordinated Rh₁ site forms an additional bond to a subsurface oxygen atom of the support, leading to a pseudo-square planar structure. The direct addition of a second CO molecule to Rh₁(CO)₁ at the 2-fold coordinated Rh₁ site to form a Rh₁(CO)₂ gem-dicarbonyl is energetically favorable according to DFT; however, this process is not observed in experiments under UHV conditions. Instead, we observe the formation of limited Rh₁(CO)₂ exclusively via the CO-induced breakup of Rh₂ dimers, in agreement with DFT results, which suggest an unstable Rh₂(CO)₃ intermediate.

1. Blum, R. *et al.* Subsurface cation vacancy stabilization of the magnetite (001) surface. *Science* **346**, 1215–1218 (2014).

8:40am **HC+SS-WeM-3 A Few Questions About Single Atom Catalysts: When Theory Helps**, *Gianfranco Pacchioni*, University of Milano-Bicocca, Italy **INVITED**

In the past, single atom catalysts (SACs) could not be clearly visualized and characterized due to the limitations associated with instrumental resolution. Today this is a new frontier in heterogeneous catalysis due to the high activity and selectivity of SACs for various catalytic reactions. This has opened various questions for theory. One is where are the atoms and what is the stability of SACs in working conditions. In order to address these questions, we will discuss the nature of isolated metal species deposited on oxide surfaces (TiO₂ and ZrO₂ in particular). These systems have been characterized experimentally using high-resolution scanning transmission electron microscopy (STEM), Fourier transform infrared spectroscopy (FTIR), and temperature programmed desorption (TPD) spectra of adsorbed CO probe molecules. Combining these data with extensive Density Functional Theory (DFT) calculations one can provide an unambiguous identification of the stable single-atom species present on these supports and of their dynamic behavior.

The other question that can be addressed by theory is the prediction of the behavior of SACs in electrocatalytic processes such as the oxygen reduction (ORR), the oxygen evolution (OER) and the hydrogen evolution (HER) reactions. In this context we assist to a rapidly growing number of DFT studies and of proposals of universal descriptors that should provide a guide to the experimentalist for the synthesis of new catalysts, in particular related to graphene-based SACs. We will critically analyze some of the current problems connected with these DFT predictions: accuracy of the calculations, neglect of important contributions in the models used, physical meaning of the proposed descriptors, inaccurate data sets used to train machine learning algorithms, not to mention some severe problems of reproducibility. It follows that the “rational design” of a catalyst based on some of the proposed universal descriptors or on the DFT screening of large number of structures should be considered with some caution.

9:20am **HC+SS-WeM-5 A Multi-Technique Study Of Ethylene and H₂ Adsorption on Rh₁/Fe₃O₄**, *Gareth Parkinson*, *C. Wang*, *P. Sombut*, *L. Puntscher*, TU Wien, Austria

The hydroformylation of alkenes has emerged as one of the most interesting applications of “single-atom” catalysis. Nevertheless, there have been relatively few fundamental studies into how the reactants (CO, alkene, and H₂) bind at the active site. In this talk I will show STM, XPS, TPD and DFT results to illustrate how C₂H₄ and H₂ interact with a Rh₁/Fe₃O₄(001) model catalyst. Ethylene binds strongly at the Rh₁ sites, but there is very little evidence for the formation of di-ethylene species under UHV conditions. H₂ adsorbs as a dihydride at the Rh₁ sites, and desorbs close to room

Wednesday Morning, November 8, 2023

temperature in TPD experiments without spilling over onto the oxide support. Evidence for the co-adsorption of the different reactants will be discussed in the context of the hydroformylation reaction.

9:40am HC+SS-WeM-6 Remote Activation of H-H bonds by Platinum in Single-Atom Alloy Catalysts, *Francisco Zaera*, University of California Riverside

With heterogeneous catalysts, chemical promotion takes place at their surfaces. Even in the case of single-atom alloys (SAA), where a reactive metal is atomically dispersed in small quantities within the main host, it is assumed that both elements are exposed and available to bond with the reactants. Here we show, on the basis of *in situ* x-ray absorption spectroscopy data, that the Pt atoms in Cu-Pt SAA catalysts are located at the inner interface between the metal nanoparticles and the silica support instead. Kinetic experiments indicated that these catalysts still display better selectivity for the hydrogenation of unsaturated aldehydes to unsaturated alcohols than the pure metals. Quantum mechanics calculations not only corroborated the particular stability of Pt at the metal-support interface, but also explained the catalytic performance improvement as due to a remote lowering of the activation barrier for the scission of the H-H bond in molecular hydrogen at Cu sites by the internal Pt atoms.

11:00am HC+SS-WeM-10 Electrifying Industrial Chemistry at the Molecular Level: Controlling the Electrocatalytic Transformation of Alcohols and Alkanes to Valuable Products, *Marcel Schreier*, University of Wisconsin-Madison **INVITED**

Producing fuels and chemicals using renewable electricity holds the promise to enable a truly sustainable circular economy based on sustainably produced carriers of electrical energy and sustainably produced chemicals. To date, the vast majority of electrocatalytic reactions are limited to the transformation of small inorganic molecules such as CO₂, H₂O, N₂, as well as the oxidation and reduction of alcohols. However, comprehensive electrification of the chemical industry will require electrocatalytic reactions that can promote the transformations of C(sp³)-H and C(sp³)-C(sp³) bonds, which are central to today's industry.

In this presentation, I will show how fundamental understanding of the interfacial processes occurring in electrocatalytic reactions can be exploited to expand the reaction scope of electrocatalysis to the transformation of complex substrates involving the controlled activation of C-H and C-C bonds. In a first step, I will show how this approach allows us to transform ethanol to ethylene oxide, an important plastic precursor. Subsequently, I will discuss methods to electrocatalytically transform inert alkanes such as methane and ethane at room temperature.

11:40am HC+SS-WeM-12 Probing Elementary Steps and Catalyst Structure Evolution: Insights into Formic Acid Conversion on Rh/Fe₃O₄(001) Model Catalysts, *Zdenek Dohnalek*, Pacific Northwest National Laboratory

Single-atom catalysis represents an exciting area of research due to the potential to qualitatively transform the activity and selectivity of supported metal catalysts. However, our fundamental understanding of their stability under reaction conditions is limited. To address this gap, we employed scanning tunneling microscopy (STM), X-ray photoelectron spectroscopy (XPS), and temperature programmed desorption (TPD). We prepared well-characterized model Rh/Fe₃O₄(001) catalysts with distinct types of Rh single-atom sites. In model catalytic studies, we investigated the effect of reactants on the structure and activity of such Rh/Fe₃O₄(001) catalysts. Formic acid, which deprotonates to surface formate and hydroxyl species, is employed as a model to follow the fate of dehydration and dehydrogenation reaction channels. We demonstrate that small amounts of Rh adatoms induce a shift from the dehydration pathway yielding CO on bare Fe₃O₄(001) to dehydrogenation yielding CO₂ on Rh_{ad}-Fe₃O₄(001). Multiple turnovers are achieved on each Rh_{ad} during the single TPD sweep. As Rh adatoms are highly unstable, we further studied the Rh stabilized in octahedral iron sites within the Fe₃O₄(001) surfaces that are stable on high surface area Rh/Fe₃O₄ catalysts. A similar shift from dehydration to dehydrogenation is observed, but much higher coverages of Rh are required. We showed that adsorbed species transiently destabilize Rh_{oct} and lead to the formation of Rh_{ad}, which is only present during the reaction. Independent studies of hydroxylated surfaces reveal that surface OHs are responsible for the Rh_{oct} destabilization and conversion to active Rh_{ad} species. Studies of elementary reaction steps and catalyst dynamics on well-defined model systems are critical for the future design of catalysts with maximum activity and selectivity.

12:00pm HC+SS-WeM-13 Hydrogen and Hydrocarbon Reactions on Single-Atom RhCu(100), *Laurin Joseph, M. Powers, J. Rosenstein, A. Utz*, Tufts University

A class of catalysts called single-atom alloys allow for the combination of a more reactive, more expensive dopant metal dispersed within a less active, more selective, and cheaper base metal. These catalysts have been well characterized and studied using techniques such as temperature programmed desorption (TPD), scanning tunneling microscopy (STM), and reflection absorption infrared spectroscopy (RAIRS). However, the detailed, molecular-level bond activation energetics and kinetics have not yet been experimentally interrogated for high-barrier reactions on these catalysts—a region where more efficient catalysts are most sorely needed.

We will present recent results that first characterize the dissociation and spillover of H resulting from both atomic and molecular H₂ adsorption on base Cu(100) and RhCu(100) single atom alloy, and then describe results from energy resolved molecular beam studies of CH₄ dissociation that quantify reaction probability as a function of energy distribution among reactant and surface degrees of freedom. We expect these studies will reveal new insights into the molecular mechanism for an important class of heterogeneously catalyzed reactions and provide new benchmarks for computational studies of single atom catalysts.

Surface Science Division

Room D136 - Session SS+2D+AS+HC-WeM

Surface Science of 2D Materials

Moderators: *Irene Groot*, Leiden University, The Netherlands, **Bo-Hong Liu**, National Synchrotron Radiation Research Center

8:00am SS+2D+AS+HC-WeM-1 Heterogeneous Photocatalysis: Alcohols on Bare and Metal-loaded TiO₂(110) and Fe₂O₃(012), *Moritz Eder*, TU Wien, Austria; *P. Petzoldt, M. Tschurl*, Technical University of Munich, Germany; *J. Pavelec, M. Schmid, U. Diebold*, TU Wien, Austria; *U. Heiz*, Technical University of Munich, Germany; *G. Parkinson*, TU Wien, Austria

We investigated the (photo)chemistry of alcohols on TiO₂(110) and Fe₂O₃(012) in ultra-high vacuum. Our studies focused on the role of the metal co-catalyst in the photocatalytic reaction by comparing the reactivity of bare and metal-loaded surfaces. We show that photocatalytic reactions are not merely a couple of redox reactions, but an interplay of thermal and photon-driven surface reactions.

Our results demonstrated that the co-catalyst plays a crucial role in the outcome of the reaction. On TiO₂(110), alcohols are oxidized to the aldehyde/ketone and hydrogen surface species upon illumination. The hydrogen surface species were thermally converted to H₂ by the co-catalyst, allowing for a steady-state photocatalytic conversion of alcohols and the continuous production of molecular hydrogen. Using mass spectrometry, we determined turnover frequencies and rate constants. The identification of surface mechanisms on Fe₂O₃ is less advanced, but there seem to be strong parallels in the photochemistry.

Our studies shed light on the fundamental processes involved in photocatalytic reactions on metal-loaded surfaces and contribute to the development of sustainable energy technologies.

8:20am SS+2D+AS+HC-WeM-2 Factors Governing the Reactivities of Transition Metal Carbides at Vapor/Solid and Liquid/Solid Interfaces, *S. Alhowity, A. Ganesan, M. Gharaee, O. Omolere, Qasim Adesope, K. Balogun, P. Chukwunenye, F. D'Souza, T. Cundari, J. Keber*, University of North Texas

Transition metal carbides are of broad interest for both heterogeneous and electro-catalysis. However, fundamental understanding of chemical factors governing reactivities and selectivities at the vapor/solid and liquid/solid interfaces remain sparse. Herein, *in situ* XPS results, electrochemical measurements, and DFT-based calculations are presented regarding the reactivities of NbC and TaC in the presence of O₂ vapor, and reactivity in solution towards the reduction of N₂ to NH₃. NbC and TaC films were

Wednesday Morning, November 8, 2023

prepared by DC magnetron sputtering deposition, then exposed to O₂ vapor at room temperature, and analyzed by *in situ* XPS without exposure to ambient. Similarly prepared samples were also analyzed by *ex situ* XRD. These data show that, although Nb and Ta have similar oxophilicities, (a) deposited NbC films contain significant amounts of Nb oxide phases throughout the film, whereas TaC films deposited under similar conditions do not, and (b) the exposure of NbC films to O₂ at 300 K results in significant Nb oxide formation, but that TaC films remain inert towards O₂ under these conditions. DFT calculations indicate that this significant reactivity difference towards O₂ is due in large part to the greater Ta-C bond strength compared to Nb-C, and in part due to the relative energetic stabilities of the corresponding oxides. Electrochemical studies show that ambient-exposed NbC, with a Nb₂O₅ surface layer, becomes reactive towards N₂ reduction to NH₃ under acidic conditions, but only after etching in NaOH to remove the surface oxide layer. Additionally, chronoamperometric data indicate that this reactive NbC surface is eventually modified under electrochemical conditions and becomes relatively inert towards N₂ reduction with time. Experiments involving *in situ* sample transfer between UHV and electrochemistry environments demonstrate that electrochemically active NbC surfaces in solution comprise Nb sub-oxide surface layers, in line with previous studies showing that effective NRR catalysts contain surface transition metal ions in intermediate oxidation states, supporting both N₂ lone pair attraction and pi-backbonding to bind and activate the NN triple bond.

Acknowledgement This work was supported in part by the UNT College of Science through COS grants 1600089 and RSG-2023-002 and in part by the NSF under grant no. DMR 2112864.

8:40am **SS+2D+AS+HC-WeM-3 Tunable Interfacial Electrochemistry at Moiré Material Interfaces, D. Kwabena Bediako**, University of California at Berkeley

INVITED

At electrode–electrolyte interfaces, crystallographic defects are frequently implicated as active sites that mediate interfacial electron transfer (ET) by introducing high densities of localized electronic states (DOS). However, conventional defects can be challenging to deterministically synthesize and control at an atomic level, challenging the direct study of how electronic localization impacts interfacial reactivity. Azimuthal misalignment of atomically thin layers produces moiré superlattices and alters the electronic band structure, in a manner that is systematically dependent on the interlayer twist angle. Using van der Waals nanofabrication of two-dimensional heterostructures, scanning electrochemical cell microscopy measurements, and four-dimensional scanning transmission electron microscopy, we report a strong twist angle dependence of heterogeneous charge transfer kinetics at twisted bilayer and trilayer graphene electrodes with the greatest enhancement observed near the ‘magic angles’. These effects are driven by the angle-dependent engineering of moiré flat bands that dictate the electron transfer processes with the solution-phase redox couple, and the structure of the relaxed moiré superlattice. Moiré superlattices therefore serve as an unparalleled platform for systematically interrogating and exploiting the dependence of interfacial ET on local electronic structure.

9:20am **SS+2D+AS+HC-WeM-5 Growth of Ultrathin Silica Films on Pt(111) and Rh(111): Influence of Intermixing with the Support, Matthias Kriinninger**, Technical University of Munich, Germany; *F. Kraushofer*, Technical University of Munich, Austria; *N. Refvik*, University of Alberta, Canada; *F. Esch*, Technical University of Munich, Germany; *B. Lechner*, Technical University of Munich, Austria

Silica is a widely used catalyst support material for clusters and nanoparticles. Understanding the relationship between these clusters and the support is challenging, however, because SiO₂ is insulating, and in most applications not crystalline which drastically limits the use of experimental techniques to those that work on insulating samples and are not diffraction-based. Several previous studies have investigated ultrathin, quasi-2D silica films on a variety of metal supports [1], which can then be measured by scanning tunneling microscopy (STM), XPS and most other surface science methods. Previous work on Pt(111) did not result in closed films, which was attributed to lattice mismatch [2]. We show that closed films can in fact be grown on Pt(111) when silica is deposited in excess, likely due to formation of a platinum silicide layer with slightly expanded lattice constant at the interface. We also report results of film growth on Rh(111), which is a near-perfect match to the lattice constant of freestanding SiO₂ films as calculated by theory. However, no high-quality films were achieved on Rh due to thermodynamic competition with a silicide.

References:

- [1] C. Büchner, M. Heyde, Two-dimensional silica opens new perspectives, *Prog. Surf. Sci.*, 92 (2017) 341-374.
- [2] X. Yu, B. Yang, J. A. Boscoboinik, S. Shaikhutdinov, and H.-J. Freund, *Appl. Phys. Lett.* 100 (2012), 151608.

9:40am **SS+2D+AS+HC-WeM-6 CO₂ Adsorption on Graphitic-Like Bilayer ZnO Film Studied by NAP-XPS, Bo-Hong Liu, S. Cheng**, National Synchrotron Radiation Research Center, Taiwan

CO₂ activation is a fundamental process in heterogeneous catalysis. ZnO-based catalyst has been extensively used in commercial methanol synthesis from CO₂ gas and the reverse water gas shift reaction. The adsorption behavior of CO₂ on the catalyst surface is pivotal to the reactivity. Whereas ZnO(0001)-Zn physisorbed or weakly chemisorbed CO₂,¹ strong chemisorption of the molecule happens on non-polar surfaces, such as ZnO(10-10), resulting in a tridentate carbonate.² In Operando TEM investigation during methanol synthesis shows that ZnO single atomic layer stacks distortedly around Cu nanoparticles via strong metal-support interaction. The lack of interlayer ordering between the layers suggests a weak interlayer interaction; therefore, each layer resembles a free-standing sheet.³ DFT modeling concluded that free-standing ZnO(0001) layer adopts an graphitic-like co-planar structure. The co-planar feature was verified experimentally for the bi-layer ZnO(0001) supported on Ag(111) and Au(111).⁴ On Au(111) substrate, TPD shows that CO₂ adsorbs on the low coordinate sites at the layer edges.⁵ In the present study, we investigate the CO₂ adsorption on bi-layer ZnO/Ag(111) film using NAP-XPS to extend the pressure condition towards reality. We found a more considerable CO₂ chemisorption at elevated pressure. The presentation will also address how the surface hydroxyl group influences CO₂ adsorption.

1. Wang, J.;Hokkanen, B.; Burghaus, U., Adsorption of CO₂ on pristine Zn–ZnO (0 0 1) and defected Zn–ZnO (0 0 1): A thermal desorption spectroscopy study. *Surf. Sci.* **2005**,577 (2-3), 158-166.
2. Schott, V.;Oberhofer, H.; Birkner, A.;Xu, M.;Wang, Y.;Muhler, M.;Reuter, K.; Wöll, C., Chemical activity of thin oxide layers: strong interactions with the support yield a new thin-film phase of ZnO. *Angewandte Chemie International Edition* **2013**,52 (45), 11925-11929.
3. Lunkenbein, T.;Schumann, J.;Behrens, M.;Schlögl, R.; Willinger, M. G., Formation of a ZnO overlayer in industrial Cu/ZnO/Al₂O₃ catalysts induced by strong metal–support interactions. *Angewandte Chemie* **2015**,127 (15), 4627-4631.
4. Tusche, C.;Meyerheim, H.; Kirschner, J., Observation of depolarized ZnO (0001) monolayers: formation of unreconstructed planar sheets. *Phys. Rev. Lett.* **2007**,99 (2), 026102.
5. Deng, X.;Sorescu, D. C.; Lee, J., Enhanced adsorption of CO₂ at steps of ultrathin ZnO: the importance of Zn–O geometry and coordination. *Phys. Chem. Chem. Phys.* **2017**,19 (7), 5296-5303.

11:00am **SS+2D+AS+HC-WeM-10 Investigation of Nitride Spintronic and Kagome-Structured Intermetallic Topological Materials Using Molecular Beam Epitaxy and Scanning Tunneling Microscopy, Arthur R. Smith**, Ohio University Physics and Astronomy Department

Owing to the overwhelming interest in topological [1] and spintronic materials [2], it is imperative to investigate these down to the atomic scale for their possible use in advanced devices. Many promising properties discovered among nitride materials, such as chemical stability and wide band gaps [3], may be combined with the equally promising aspects of topological materials, such as the topological Hall and Nernst effects [4]. Very recent work illustrates that spin-polarized scanning tunneling microscopy is a powerful tool for exploring topological band-structured Kagome antiferromagnets [5]. In our current work, we investigate both nitride material systems grown using molecular beam epitaxy as well as the growth of topological systems such as Kagome antiferromagnetic materials. Ongoing work in our group encompasses the investigation of Mn₃Sn, FeSn, CrSn, Mn₃Ga, and as a spintronic and topological nitride, Mn₃GaN. These materials are grown in combined UHV MBE and scanning tunneling microscopy chamber systems in which the grown samples are first fabricated using MBE and after that investigated for their structural, electronic, and magnetic properties including using STM and tunneling

Wednesday Morning, November 8, 2023

spectroscopy. Our goal is also to investigate these materials using spin-polarized STM as a function of temperature and applied magnetic field. Our current results show that these materials can be fabricated effectively using molecular beam epitaxy and investigated using various *in-situ* techniques such as reflection high energy electron diffraction and STM. Results from multiple on-going investigations will be presented with a birds-eye view of the progress. Especially to be presented will be STM and STS results in these Kagome systems grown using MBE.

This work is supported by the U.S. Department of Energy, Office of Basic Energy Sciences, Division of Materials Sciences and Engineering under Award No. DE-FG02-06ER46317.

[1] P. Liu *et al.*, "Topological nanomaterials," *Nat. Rev. Mater.* **4**, 479 (2019).

[2] A. Hirohata *et al.*, "Review on spintronics: Principles and device applications," *Journal of Magnetism and Magnetic Materials* **509**, 166711 (2020).

[3] M. Xu *et al.*, "A review of ultrawide bandgap materials: properties, synthesis and devices," *Oxford Open Materials Science* **2**(1), itac004 (2022).

[4] S. Roychowdhury *et al.*, "Giant Topological Hall Effect in the Noncollinear Phase of Two-Dimensional Antiferromagnetic Topological Insulator MnBi₄Te₇," *Chemistry of Materials* **33**, 8343 (2021).

[5] H. Li *et al.*, "Spin-polarized imaging of the antiferromagnetic structure and field-tunable bound states in kagome magnet FeSn," *Scientific Reports* **12**, 14525 (2022).

11:20am **SS+2D+AS+HC-WeM-11 Molecular Beam Epitaxial Growth and Investigations of FeSn on LaAlO₃**, Tyler Erickson, S. Upadhyay, H. Hall, D. Ingram, S. Kaya, A. Smith, Ohio University

Kagome antiferromagnetic and ferromagnetic materials provide an interesting avenue for research through the investigation of frustrated magnetism, band topology and electronic correlations [1-4]. FeSn is a layer-wise antiferromagnetic Kagome structured material with characteristic dispersion-less flat bands and Dirac cones at the Brillouin zone boundaries. Li *et al.* have presented exciting spin-polarized scanning tunneling microscopy results revealing surface electronic and magnetic properties of *in-situ* cleaved bulk FeSn [1]. Zhang *et al.* reported strain engineering of FeSn on SrTiO₃ (111) with precise control of the stanene layers [2]. Kawakami *et al.* reported Fe₃Sn₂ growth on Pt buffer layers on top of Al₂O₃ and studied various topological phenomena of this topological Kagome material [3,4]. Bhattarai *et al.* studied the magnetotransport properties of FeSn grown on silicon substrates [5]. Here, we study the growth of FeSn directly on LaAlO₃ and report the successful growth of high-quality crystalline thin-films of FeSn. Reflection high-energy electron diffraction and x-ray diffraction are used to discover the *in-plane* and *out-of-plane* lattice constants, while atomic force microscopy and Rutherford backscattering provide topographical and stoichiometric characterization. Preliminary results indicate *in-plane* and *out-of-plane* lattice constants of 5.290 Å and 4.56 Å compared to the expected results of 5.297 Å and 4.481 Å, respectively. Besides discussing the thin film FeSn growth results, we also plan to present scanning tunneling microscopy results on the MBE-grown surfaces.

This work is supported by the U.S. Department of Energy, Office of Basic Energy Sciences, Division of Materials Sciences and Engineering under Award No. DE-FG02-06ER46317.

[1] H. Li *et al.*, *Scientific Reports*, 12 14525 (2022)

[2] H. Zhang *et al.*, *Nano Lett.* **23**, 239 – 2404 (2023)

[3] I. Lyalin *et al.*, *Nano Lett.* **21**, 6975 – 6982 (2021)

[4] S. Cheng *et al.*, *APL Mater.* **10**, 061112 (2022)

[5] N. Bhattarai *et al.*, *Phys. Status Solidi A*, **220**: 2200677 (2023)

11:40am **SS+2D+AS+HC-WeM-12 AVS Graduate Research Awardee Talk: Molecular Beam Epitaxial Growth, Structural Properties, and Surface Studies of a-Plane-Oriented Mn₃Sn on C-Plane Al₂O₃**, Sneha Upadhyay¹, T. Erickson, Ohio University; J. Hernandez, Universidad Autonoma de Puebla, Mexico; H. Hall, K. Sun, Ohio University; G. Cocoltzi, Universidad Autonoma de Puebla, Mexico; N. Takeuchi, Universidad Nacional Autonoma de Mexico, Mexico; A. Smith, Ohio University

Recently, Chen *et al.* reported the observation of tunneling magnetoresistance in an all-antiferromagnetic tunnel junction consisting of Mn₃Sn/MgO/Mn₃Sn.¹ Furthermore, Bangar *et al.* demonstrated a technique for engineering the spin Hall conductivity of Mn₃Sn films by changing the Mn: Sn composition.² These works show the potential of studying this Kagome antiferromagnetic material and the importance of being able to grow smooth films. This work uses molecular beam epitaxy to investigate the growth of Mn₃Sn (11 $\bar{2}$ 0) on Al₂O₃ (0001). The growth is monitored *in-situ* using reflection high energy electron diffraction and measured *ex-situ* using X-ray diffraction, Rutherford backscattering, and atomic force microscopy. In our previous work, we carried out a single-step growth at 450°C, which resulted in a crystalline but discontinuous *a-plane-oriented* (~43% 11 $\bar{2}$ 0) Mn₃Sn film with a mix of other orientations including 0002.³ Leading from this work, changes were made to the growth recipe, which involved carrying out a two-step growth procedure at room temperature, resulting in a contiguous, epitaxial Mn₃Sn film with up to ~82% 11 $\bar{2}$ 0-orientation. We are also exploring the effect of varying the Mn: Sn flux ratio and the film thicknesses (in the range of 5 – 200 nm) on the film crystallinity and orientation. We observe that varying the Mn: Sn flux ratio leads to a change in the RHEED patterns from pointy to streaky, and the XRD shows that the 11 $\bar{2}$ 0 peak can be varied between ~82% to ~38% of all the peaks' total intensity. We also plan to present the first results on ultra-high vacuum scanning tunneling microscopy imaging of the (11 $\bar{2}$ 0) Mn₃Sn surface.

Acknowledgments:

The authors acknowledge support from the U.S. Department of Energy, Office of Basic Energy Sciences, Division of Materials Sciences and Engineering under Award No. DE-FG02-06ER46317. The authors would like to thank Dr. Eric Stinoff and his students for back-coating the sapphire (0001) substrates.

¹ X. Chen *et al.*, "Octupole-driven magnetoresistance in an antiferromagnetic tunnel junction." *Nature* **613**, 490 (2023).

² H. Bangar *et al.*, "Large Spin Hall Conductivity in Epitaxial thin films of Kagome Antiferromagnet Mn₃Sn at room temperature", *Adv. Quantum Technol.* **6**, 2200115 (2023).

³ S. Upadhyay *et al.*, "Molecular beam epitaxy and crystal structure of majority *a-plane* oriented and substrate strained Mn₃Sn thin films grown directly on sapphire (0001)", *Journal of Vacuum Science and Technology A*, to be published (2023).

Wednesday Afternoon, November 8, 2023

Fundamental Discoveries in Heterogeneous Catalysis Focus Topic

Room B113 - Session HC+SS-WeA

Advances in Complex Catalytic Systems

Moderators: Zdenek Dohnalek, Pacific Northwest National Laboratory, **Dan Killelea**, Loyola University Chicago

2:20pm **HC+SS-WeA-1 Computational Studies of Selective Reduction Reactions on Metal and Metal Compounds Electrocatalysts**, *J.R. Schmidt*, UW Madison **INVITED**

Understanding and controlling the factors that govern selectivity in electrocatalysis is key to enabling a wide range of electrochemical transformations. I will highlight efforts from two ongoing collaborative studies, focusing on the selective 2e⁻ reduction of oxygen to hydrogen peroxide over a series of transition metal dichalcogenides; and the selective reduction of highly functionalized biomass molecules using traditional metallic electrocatalysts. In both cases, I will demonstrate how emerging computational electrocatalysis approaches yield a rich picture for the factors that govern catalytic selectivity in these systems. In addition, I will briefly discuss recent work focused on increasing the long-term stability of these electrocatalysts, opening the doors to potential commercial applications.

3:00pm **HC+SS-WeA-3 Metal Atom Chemical Potential: A Key Descriptor for Predicting Particle Size Effects on Catalyst Performance, and How to Estimate It**, *Charles T. Campbell*, *K. Zhao*, *N. Janulaitis*, University of Washington

Many important catalysts and electrocatalysts for energy and environmental technologies involve late transition metal nanoparticles dispersed across the surface of some oxide or carbon support. The activity and long-term stability of these materials depend strongly on particle size below 7 nm, and, in this size range, upon the composition and atomic-level structure of the support surface. We show here that the chemical potential of the metal atoms in such supported catalysts provides a convenient descriptor of their performance as heterogeneous catalysts that captures many of the effects of particle size, metal-metal alloying and support on catalyst performance. Based on microcalorimetric measurements of metal adsorption energies, the metal chemical potential is shown to be predictable as a function of metal particle size and the adhesion energy of the particle to the support. For oxide supports, this adhesion energy correlates predictably with metal oxophilicity, as we defined based on heats of oxide formation from gaseous metal atoms. For carbon supports, this adhesion energy correlates predictably with metal carbophilicity, as we defined based on DFT estimates of C atom adsorption energies. These correlations provide predictions of metal chemical potential that can enable catalyst design.

Work supported by DOE-OBES under Grant Number DE-FG02-96ER14630.

3:20pm **HC+SS-WeA-4 Size-Dependent Properties of Cobalt Nanoclusters on CeO₂(111)**, *M. Rahman*, Louisiana State University; *T. Ara*, University of Wyoming; *Ye Xu*, Louisiana State University; *J. Zhou*, University of Wyoming
Cobalt is a versatile catalytic metal. It has been used to catalyze many reactions of technological importance, including Fischer-Tropsch synthesis, reforming, and ammonia synthesis, where oxidic Co and metallic Co lead to different catalytic pathways. Meanwhile, ceria offers a desirable set of properties as catalyst support, including the abilities to stabilize nanoclusters, undergo redox interaction with metals, and enhance oxygen availability. Nanoparticles of Co supported on ceria have therefore been the mainstay of many heterogeneous catalysis studies. We have carried out an investigation of Co nanoclusters supported on stoichiometric CeO₂(111) using computational modeling and scanning tunneling microscopy (STM). Various sizes up to ca. 20 Co atoms have been optimized using a minima hopping algorithm combined with density functional theory (DFT) calculations, which identifies many compact, symmetric structures as minimum-energy for the sizes that are considered. Theory predicts that in this size regime, the Co clusters prefer to be notably wider than they are high. A significant fraction of the Co atoms in each cluster are oxidized, and most of those are located on the periphery between the clusters and ceria. Co atoms that are not directly in contact with the surface are effectively screened and remain neutral. The large aspect ratios and high fractions of oxidic Co in small clusters at low Co metal coverages are corroborated by STM studies of Co deposited on CeO₂(111) thin film surfaces at ambient

temperature. Our findings shed light on atomic-level characteristics of Co nanoclusters on ceria that are relevant to catalytic applications.

4:20pm **HC+SS-WeA-7 on-Surface Synthesis of Porous Planar-Carbon-Lattices: Fundamental Properties and Applications**, *Abner de Siervo*, Institute of Physics Gleb Wataghin, University of Campinas (UNICAMP), Brazil **INVITED**

Materials science in the nanoscale domain has become a reality for several applications, from integrated circuits, sensors, catalysts, medicines, and data-storage devices, among others [1]. We achieved the ability to understand materials and, more importantly, command the materials' properties at the atomic level using precise synthesis and growth methods. Therefore, during the last decades, enormous efforts have been made to develop new processes for the fabrication, characterization, and manipulation of materials in complex nanoarchitectures with atomic precision, making it possible to express emergent new chemical, electronic, photonic, magnetic, and structural properties. On-surface synthesis becomes a powerful bottom-up technique to fabricate such nanostructures using organic and organometallic precursors as molecular building blocks [2]. In this talk, I will present some strategies we have adopted to produce planar carbon lattices nanostructures, for example, porous nanoribbons and nanomembranes [3-5]. For a complete understanding of the atomic and electronic properties of the materials, we have combined scanning tunneling microscopy and spectroscopy (STM/STS), X-ray photoelectron spectroscopy (XPS), and numerical simulations based on density functional theory (DFT) calculations.

Acknowledgments:

FAPESP, CNPq, and CAPES from Brazil have financially supported this work.

References:

- [1] G Ali Mansoori and TA Fauzi Soelaiman. Nanotechnology—An introduction for the standards community. ASTM International, 2005.
- [2] Johannes V. Barth. Annual Review of Physical Chemistry, 58(1):375–407, 2007.
- [3] Alisson Ceccatto dos Santos, et al., Chemistry of Materials 32 (5), 2114–2122 (2020).
- [4] Nataly Herrera-Reinoza, et al., Chemistry of Materials 33, 2871–2882 (2021).
- [5] Alisson Ceccatto dos Santos, et al., J. Phys. Chem. C 125, 31, 17164–17173 (2021).

5:00pm **HC+SS-WeA-9 2D Surface Optical Reflectance for Surface Studies in Harsh Environments**, *A. Larsson*, Lund University, Sweden; *S. Pfaff*, Sandia National Laboratories; *L. Ramisch*, *S. Gericke*, *A. Grespi*, *J. Zetterberg*, *Edvin Lundgren*, Lund University, Sweden

During recent years, 2D Surface Optical Reflectance (2D-SOR) [1,2] microscopy [3] has emerged as a valuable surface characterization tool for model catalysts or electrodes [4] when performing operando investigations in harsh environments. In particular, 2D-SOR microscopy is favorably used as a complementary technique to other photon-in-photon-out techniques which do not carry direct information on the surface 2D morphology. In this presentation we will present the development and examples of 2D-SOR instrumentation and investigations from single and poly-crystalline samples in combination with Planar Laser Induced Fluorescence (PLIF) [2, 3], High Energy Surface X-Ray Diffraction (HESXRD) [5,6,7] and Polarization Modulation-Infrared Reflection Absorption Spectroscopy (PM-IRRAS) [8] coupled to Mass Spectrometry (MS) and Cyclic Voltammetry (CV) in thermal catalysis, electrocatalysis and corrosion. Illustrating examples of the versatility of the technique will be shown including reflectance changes during the thermal CO oxidation over Pd(100) and Pd polycrystalline

Wednesday Afternoon, November 8, 2023

surfaces. We show that reflectance changes during the reaction can be associated with the formation of thin Pd oxides by the combination of 2D-SOR and Surface X-Ray Diffraction (SXRD). The combined measurements demonstrate a sensitivity of 2D-SOR to the formation of a 2-3 Å thin Pd oxide film. During Cyclic Voltammetry (CV) in an acidic electrolyte using a Au(111) surface as an electrode, we show that the differential of the change in 2D-SOR reflectance correlate to various current features in the CV curve. This observation can be used to differentiate current features in the CV curve from a polycrystalline Au surface, demonstrating that the different grains contribute to the current at different potentials due to the different surface orientations. Finally, we show that 2D-SOR is a cheap and useful technique to investigate the corrosion of applied materials such as duplex stainless steels and Ni alloys.

- [1] W. G. Onderwaater et al Rev. Sci. Instrum., **88** (2017) 023704.
- [2] J. Zhou et al, J. Phys. Chem. C **121** (2017) 23511.
- [3] S. Pfaff et al, ACS Appl. Mater. Interfaces **13** (2021) 19530.
- [4] W. Linpe, et al, Rev. Sci. Instrum., **91** (2020) 044101.
- [5] S. Pfaff, et al Rev. Sci. Instrum. **90** (2019) 033703.
- [6] S. Albertin, et al, J. Phys. D: Appl. Phys. **53** (2020) 224001.
- [7] W. Linpé, et al J. Electrochem. Soc. **168** (2021) 096511.
- [8] L. Rämisch et al, Appl. Surf. Sci. **578** (2022) 152048

5:20pm **HC+SS-WeA-10 Interrogating Reactive Sites with Intrinsic Kinetics Over Well-Defined Supported Pt Nanoparticles**, *T. Kim, C. O'connor, Christian Reece*, Harvard University

The chemical industry is the primary consumer of energy and fossil fuels in the industrial sector and relies almost entirely on complex heterogeneous catalytic systems. Yet our ability to employ these systems far outweighs our understanding. While a detailed understanding of heterogeneous catalysts does exist for model systems (e.g., 2D single crystals) at ultra-high vacuum, our understanding of applied catalytic materials (e.g., metal nanoparticles deposited on a metal oxide support) under reaction conditions is still lacking. Herein we utilize the Temporal Analysis of Products (TAP) technique to precisely resolve the intrinsic kinetics of CO oxidation of size selected 2nm Pt nanoparticles supported on SiO₂. Using Diffuse Reflectance Infrared Fourier Transform Spectroscopy (DRIFTS) we identify multiple types of well-coordinated, undercoordinated, and bridge-bound CO sites exist on the Pt nanoparticles. However, through a combination of isotopic labelling and microkinetic modelling, we find that only two pathways for CO oxidation exist over the catalyst surface under the entire range of reaction conditions studied: a fast and a slow pathway. The fast pathway follows typical catalytic behaviour and shows a strong temperature dependence and a linear dependence on CO coverage, but the slow pathway is independent of both temperature and CO coverage which is unexpected for a slow catalytic process. This study demonstrates the importance of being able to precisely resolve kinetics over applied catalytic materials using techniques such as TAP. Further, it also hints that under reaction conditions the highly dynamic nature of catalytic surfaces implies that our classical understanding of structure-activity-relationships may not hold as strong as originally hoped.

5:40pm **HC+SS-WeA-11 The Effects of Catalytic Cluster Size on Catalysis and Electrocatalysis**, *Scott Anderson*, University of Utah **INVITED**

Supported sub-nano clusters are potentially a metals-efficient approach to catalysis, where all the expensive catalytic atoms (Pt, Pd, etc.) are exposed in the surface layer. In addition, because the properties of small clusters are highly size dependent, varying the cluster size provides a parameter that can be used to tune activity and selectivity. The problem with small clusters is that they tend to sinter and poison easily, and much of our work is in developing approaches to stabilize the supported clusters under thermal or electro-catalytic conditions.

Deposition of mass-selected clusters in UHV is used to prepare model catalysts and electrocatalysts with catalytic centers that all start out being the same size. We have developed an in-vacuum ALD-like self-limiting reaction approach to dope or alloy the clusters with elements like B, Sn, or Ge, with the goal of stabilizing the clusters against both poisoning and sintering. Two types of catalysis experiments will be described.

Gas-surface catalysis is studied in the UHV system by mass spectrometric methods, but we also have new microreactor system that allows clusters deposited on alumina or silica surfaces to be exposed to reactant flows at pressures up to 1 atm, with mass spectrometric product detection. This part of the talk will focus on using Ge doping to stabilize small Pt clusters against deactivation by both carbon deposition (coking) and sintering at

temperatures up to 700 K. To goal is to make stable and selective alkane dehydrogenation and cracking catalysts.

Electrocatalysis is studied either *in situ*, using an electrochemical cell housed in an antechamber to the UHV system, or in conventional benchtop electrochemical cells. The *in situ* experiments allow us to study aqueous electrochemistry with minimal air exposure, while the *ex situ* setups allow more elaborate types of electrochemical measurements. Results for the hydrogen evolution reaction (HER), oxygen evolution reaction (ORR), and alcohol electro-oxidation will be presented for catalytic Pt_n clusters deposited on indium tin oxide (ITO), fluorine tin oxide (FTO), and graphite (HOPG). For ITO/FTO, electrodes were prepared by soft landing the clusters. For HOPG, the effects of deposition energy on electrocatalytic activity and stability, and on physical properties measured by XPS and ISS will be discussed.

Fundamental Discoveries in Heterogeneous Catalysis Focus Topic

Room B113 - Session HC+SS-ThM

Dynamics and Mechanisms in Heterogeneously Catalyzed Reactions

Moderators: Arthur Utz, Tufts University, Jason Weaver, University of Florida

8:00am **HC+SS-ThM-1 Dehydration and Dehydrogenation of Formate on Fe₃O₄(001)**, Marcus Sharp, Pacific Northwest National Laboratory / Washington State University; C. Lee, S. Smith, B. Kay, Z. Dohnálek, Pacific Northwest National Laboratory

Interest in improving the activity and selectivity of catalysts has been persistent due to their importance in numerous chemical industries. Yet the mechanistic understanding of the active site structure, coordination environment, and stability is often lacking. Using a combination of temperature programmed reaction spectroscopy (TPRS), molecular beam scattering (MBS), and X-ray photoelectron spectroscopy (XPS) we investigate the reactivity of formic acid on the Fe₃O₄(001) that serves as a model reducible oxide support for single-atom catalysts. XPS shows that formic acid deprotonates at low temperature (~80 K), forming a formate intermediate and a protonated lattice oxygen (hydroxyl). At higher temperatures (400–600 K), the formate undergoes dehydration to CO and H₂O via two desorption channels, while dehydrogenation to CO₂ is a minor channel. Angle-resolved TPRS and MBS experiments show that CO leaves the surface with excess kinetic energy closely focused along the surface normal. Surprisingly, not all formate species can react through the low-temperature channel. XPS, however, does not indicate a change in surface species throughout reaction temperatures. The addition of isotopically labeled formic acid (DCOOD) after the depletion of the low-temperature reaction channel show a complete mixing of all surface formate species. Similarly, the addition of atomic hydrogen after the depletion of the low-temperature reaction shows that surface hydroxyls are important in guiding the decomposition reaction to various reaction channels. Fe deposition on top of Fe₃O₄(001) reveals that Fe based-structures also act as the active sites for the high-temperature desorption of CO. This study illustrates the complexity of reaction intermediates at catalyst surfaces where changes in surface morphology can lead to differences in product selectivity and activity.

8:20am **HC+SS-ThM-2 The Effect of No and Co on the Rh(100) Surface at Atmospheric Pressure**, D. Boden, J. Meyer, Irene Groot, Leiden University, Netherlands

Rhodium is used in automotive catalysis to reduce NO and CO emissions in the exhaust by catalyzing the reduction of NO to N₂ and the oxidation of CO to CO₂. This means the rhodium nanoparticles in the catalyst are exposed to high pressures of NO and CO, both known to be highly corrosive gases, which leads to disintegration and sintering of the rhodium catalyst. It is important to understand the effect high pressures of NO and CO have on the rhodium surface at the nano scale, in order to design strategies to impede catalyst deactivation. Here, one of the most active rhodium facets, Rh(100), is studied at atmospheric pressures of NO and CO with scanning tunnelling microscopy (STM), in order to observe the roughening of the surface *in situ*. Additionally, atomistic thermodynamics, based on density functional theory (DFT) calculations, is used in combination with *ex situ* ultrahigh vacuum techniques (low-energy electron diffraction and Auger electron spectroscopy) to understand the behavior of adsorbates on the surface during the STM experiments, at the atomic scale. The formation of rhodium islands on the (100) terraces is observed at high CO pressures, in conjunction with roughening of the step edges. Interestingly, roughening does not occur at the same pressures of NO. The surface roughening is also less severe when co-dosing NO and CO, even at identical CO partial pressures. The results from atomistic thermodynamics show that NO likely inhibits CO adsorption by blocking the CO adsorption sites, thereby preventing carbonyl formation and decreasing surface roughening.

8:40am **HC+SS-ThM-3 Sustainable Production of Aromatics via Methane Dehydroaromatization: Role of Dynamic Carbon Accumulation**, M. Hossain, Virginia Tech; M. Rahman, Southwest Research Institute, San Antonio Texas; D. Maiti, E. Sobchinsky, M. Kunz, R. Fushimi, Idaho National Laboratory; **Sheima Khatib**, Virginia Tech **INVITED**

Natural gas, mainly composed of methane, constitutes an available and cheap resource that can be used as a building block to produce chemicals. Methane dehydroaromatization (MDA) is a reaction capable of directly converting methane to value-added aromatics, without an intermediate syngas step. The reaction happens in non-oxidative conditions, producing mainly benzene and hydrogen, $6 \text{CH}_4(\text{g}) \rightarrow \text{C}_6\text{H}_6(\text{g}) + 9\text{H}_2(\text{g})$. Zeolite-supported Mo catalysts have so far been the most widely studied catalysts in MDA, but they do not fulfill the conversion and stability requirements for commercialization. During the reaction induction period, Mo oxide species gradually reduce to Mo carbides, which are responsible for methane activation and subsequent conversion to aromatics. We have developed a strategy to improve benzene yield and catalyst stability by controlling the activation of the Mo species to optimize their reduction and dispersion before exposure to reaction conditions. Our results indicate that when activation of catalysts is performed by reduction in pure hydrogen under temperature-controlled conditions, the carbides formed (*ex situ*) lead to more selective catalysts that deactivate more slowly compared to carbides formed during reaction (*in situ*). To explain this difference, we studied the dynamic carbon accumulation kinetics on varying redox states of MoOx/HZSM-5 catalyst via strategic molecular probe experiments in the Temporal Analysis of Products (TAP) reactor. Incremental pulse-by-pulse TAP investigation helps to distinguish different surface reactions and paves the way for elucidating the role of catalyst state towards preferential soft coke formation, as opposed to hard coke that results in catalyst deactivation. These intrinsic kinetic fingerprints of the catalyst will provide guidance towards better MDA reaction protocols for sustained high aromatics production from waste greenhouse gas, methane.

9:20am **HC+SS-ThM-5 Mechanistic Understanding of Methanol Synthesis on an In₂O₃ Catalyst**, Yong Yang, ShanghaiTech University, China

Indium oxide (In₂O₃) became a very promising catalyst in recent years for its high selectivity of CO₂ hydrogenation to methanol, an ideal fuel for green energy. The reaction normally requires elevated temperature from 220 to 330°C and relative high pressure around 50 bar. Deep mechanistic insight with experimental evidence is still in demand for effective development in catalyst rational design. The widely applied direct kinetics investigation by *in situ* IR of this reaction is difficult due the formation of In₂O₃ black under H₂ reduction condition.

Here based on a recent optimized c-In₂O₃ catalyst, we investigate methanol synthesis reactivity correlated spectroscopic and kinetics properties at up to 16 bar and 270°C by online MS isotope kinetics measurements, *in situ* time resolved FT-IR and XPS (ThermoFisher ESCALab250Xi), in both in steady-states and transients. In all kinetics experiments reported here, the input total flow rate is controlled around 15 sccm with H₂/D₂:CO₂:Ar ratio at 10.5 sccm:3.5 sccm:1.4 sccm and the resulted gas hour space velocity is around 17 L/g/Hr.

Both steady-states and transients isotope input results clearly indicate a normal kinetic isotope effect (KIE). In addition pressure dependence study indicates that the reaction rate is nearly proportional to the input pressure and Arrhenius plot yield activation energies with both inputs remain almost constant at different pressures, with a higher activation energy (E_a) for D₂/CO₂ than H₂/CO₂ (120 vs. 100 kJ/mol). The KIE and pressure dependence behaviors are essentially different from Cu based catalyst in the same reaction, although E_a values are close. A universal reaction rate equation with parameters of pressure and temperature is thus provided. Based on results from two series of isotope switching transients experiments from D₂/CO₂ to H₂/CO₂, quantitative transient products analysis of exchanged D/H isotopic species reveals that there are up to 2.5 monolayers of dissociated deuterium involves in the D isotopomer methanol products. This indicates that the active surface is highly reduced with a high efficiency of surface hydrogenation to methanol. The surface species characterization by *in situ* FT-IR and XPS investigate sample *in situ* prepared as pre-oxidized, pre-reduced and further exposed with water vapor or CO₂. The combined results provide key evidence for main XPS features assignments.

These results helps elucidating the kinetics and spectroscopic fundamentals in this reaction and hopefully will provide useful information toward the rational design of active and stable catalysts based on In₂O₃ for CO₂ hydrogenation to methanol.

Thursday Morning, November 9, 2023

9:40am **HC+SS-ThM-6 The Strong Metal-Support Interaction Under Reactive Conditions and Its Influence on the Hydrogen Evolution Reaction Over Pt/TiO₂(110)**, *Philip Petzoldt*, Technical University of Munich, Germany; *M. Eder*, TU Wien, Austria; *M. Blum*, Lawrence Berkeley National Laboratory (LBNL); *T. Kratky*, Technical University of Munich, Germany; *S. Günther*, Technical University Munich, Germany; *M. Tschurl*, *B. Lechner*, *U. Heiz*, Technical University of Munich, Germany

Covering reactive nanoparticles with thin metal oxide films is a promising strategy to improve their stability and catalytic selectivity. Reductive heating of noble metal particles supported on reducible oxides initiates their encapsulation due to the strong metal-support interaction (SMSI). This phenomenon has been studied under well-defined UHV conditions on single crystals and on more applied, structurally inhomogeneous catalysts. However, only few studies provide insight at the atomic scale under reactive conditions which is crucial for the systematic optimization of catalytic systems.

In this contribution, we investigate the dynamic behavior of the SMSI state on Pt-loaded TiO₂(110) under reactive conditions and its influence on the catalyst's activity in the photocatalytic hydrogen evolution reaction. Employing near ambient pressure XPS, we show that the SMSI kinetics may be tuned by choosing the oxygen pressure. Monitoring the hydrogen evolution reaction by mass spectrometry, we further demonstrate that the impact of the noble metal encapsulation on the catalyst's chemistry depends on the complex interplay of reaction conditions and catalyst preparation.

Our results provide new mechanistic insights into the interaction of noble metal particles with the support and may foster the development of catalysts with improved stability and selectivity.

11:00am **HC+SS-ThM-10 Rotational Orientation Effects in Hydrogen-Surface Scattering**, *Helen Chadwick*, *Y. Alkoby*, *G. Alexandrowicz*, Swansea University, UK

INVITED

The interaction of hydrogen with surfaces plays an important role in many heterogeneously catalysed reactions, for example converting ortho-hydrogen to para-hydrogen for the safe storage of liquid H₂ fuel, in the Haber Process for making ammonia and in the Fischer-Tropsch synthesis for making longer chain hydrocarbons. Carefully controlled, quantum state resolved experiments play a pivotal role in providing benchmarks which can be used to help develop accurate, predictive theoretical models of these important interactions. The influence of the rotational orientation projection quantum state of the molecule (m_j), which can be considered classically to describe whether the hydrogen is rotating like a helicopter or cartwheel when it collides with the surface, has been less well characterised due to the challenges associated with preparing these quantum states, particularly in closed shell, ground state molecules. Here I will present a unique magnetic manipulation interferometry technique [1] that allows us to control and manipulate the rotational orientation and nuclear spin projection (m_j) quantum states of small molecules both before and after they collide with a surface. Using the elastic scattering of H₂ from LiF as an example [2], I will demonstrate that we can extract empirical scattering matrices from the data which can be compared directly to those from theoretical calculations. I will also show new results for H₂ scattering from the stepped Cu(511) surface, where signals for several different diffraction channels have been measured which exhibit different dependencies on the rotational orientation states, as well as observations which suggest that H₂ can dissociate when it collides with the surface. All of these results combined, provide very stringent experimental benchmarks which will help develop accurate theoretical models.

Acknowledgments: This work was supported by the Horizon 2020 Research and Innovation Programme Grant Number 772228 and an EPSRC New Horizons Grant Number EP/V048589/1.

References

- [1] O. Godsi et al., Nat. Comm. 8, 15357 (2017).
- [2] Y. Alkoby et al., Nat. Comm. 11, 3110 (2020).

11:40am **HC+SS-ThM-12 Studies of Pt-Sn Catalysts for Methylcyclohexane Dehydrogenation to Toluene**, *Donna Chen*, University Of South Carolina; *M. Qiao*, *A. Ahsen*, *A. Heyden*, *J. Monnier*, University of South Carolina
The use of H₂ as an energy carrier has emerged as an attractive alternative to fossil fuels, but a major challenge for the H₂-based economy lies in the efficiency of storage and transportation. The use of liquid organic hydrogen carriers (LOHC) would allow for the reversible storage of H₂ through hydrogenation-dehydrogenation reactions. The toluene-methylcyclohexane (MCH) pair is ideal for this purpose because MCH has a relatively high

gravimetric storage density, and both compounds are widely available, low-toxicity liquids at ambient temperature. While catalytic hydrogenation of LOHCs is exothermic and facile, a major problem with using LOHCs for hydrogen storage is that catalytic dehydrogenation is endothermic and not always reversible due to side reactions. Pt catalysts are active for dehydrogenation of MCH to toluene, but undesirable C-C bond breaking reactions also lead to coking and deactivation. In this work, model Pt-Sn bimetallic surfaces are studied for MCH dehydrogenation in order to understand the role of Sn in preventing the deactivation of Pt surfaces. Pt-Sn alloy surfaces were prepared by depositing Sn on Pt(111) and annealing to various temperatures to form ordered overlayers, which were characterized by low energy electron diffraction, scanning tunneling microscopy (STM), and X-ray photoelectron spectroscopy (XPS) in an ultrahigh vacuum (UHV) chamber. The model surfaces were then transferred into a flow reactor coupled directly to the UHV chamber for kinetic studies under realistic pressure conditions; after MCH reaction, the surfaces were transferred back to the UHV chamber for characterization by XPS and STM. The activity of the model single-crystal surfaces are also compared with the conventional catalysts consisting of supported Pt-Sn particles. Computational work will help identify the role of the various active sites and determine reaction mechanisms, as well as the rate and selectivity controlling steps at the active sites.

12:00pm **HC+SS-ThM-13 Platinum@Hexaniobate Nanopeapods: A Directed Photocatalytic Architecture for Dye-Sensitized Semiconductor H₂ Production Under Visible Light Irradiation**, *Clare Davis-Wheeler Chin*, Sandia National Laboratories, USA; *P. Fontenot*, Tulane University; *T. Rostamzadeh*, University of New Orleans; *L. Treadwell*, Sandia National Laboratories, USA; *R. Schmehl*, Tulane University; *J. Wiley*, University of New Orleans

Platinum@hexaniobate nanopeapods (Pt@HNB NPPs) are a nanocomposite heterogeneous photocatalyst that was selectively engineered to increase the efficiency of hydrogen production from visible light photolysis. Pt@HNB NPPs consist of linear arrays of high surface area Pt nanocubes encapsulated within scrolled sheets of the semiconductor H_xK_{4-x}Nb₆O₁₇, and were synthesized in high yield via facile one-pot microwave heating method that is fast, reproducible, and more easily scalable than multi-step approaches required by many other state-of-the-art catalysts. The Pt@HNB NPPs unique 3D architecture enables physical separation of the Pt catalysts from competing surface reactions, promoting electron efficient delivery to the isolated reduction environment along directed charge transport pathways that kinetically prohibit recombination reactions. Pt@HNB NPPs catalytic activity was assessed in direct comparison to representative state-of-the-art Pt/semiconductor nanocomposites (extPt-HNB NSCs) and unsupported Pt nanocubes. Photolysis under identical conditions exhibited superior H₂ production by the Pt@HNB NPPs, which exceeded other catalyst H₂ yields (μmol) by a factor of 10. Turnover number (TON) and apparent quantum yield (AQY) values showed similar dramatic increases over the other catalysts. Overall, the results clearly demonstrate that Pt@HNB NPPs represent a unique, intricate nanoarchitecture among state-of-the-art heterogeneous catalysts, offering obvious benefits as a new architectural pathway towards efficient, versatile, and scalable hydrogen energy production. Potential factors behind the Pt@HNB NPPs superior performance are discussed below, as are the impacts of systematic variation of photolysis parameters and the use of a non-aqueous reductive quenching photosystem.

Funding Statement

This material is based upon work supported by the National Science Foundation under grants CHE-1412670 (C.D.-W.C., T.R., J.B.W) and CHE-2004178 (J.B.W). Work is also supported by the Laboratory Directed Research and Development program at Sandia National Laboratories (C.D.-W.C., L.J.T.), a multimission laboratory managed and operated by National Technology and Engineering Solutions of Sandia LLC, a wholly owned subsidiary of Honeywell International Inc. for the U.S. Department of Energy's National Nuclear Security Administration under contract DE-NA0003525. (This paper describes objective technical results and analysis. Any subjective views or opinions that might be expressed in the paper do not necessarily represent the views of the U.S. Department of Energy of the United States Government).

Thursday Afternoon, November 9, 2023

Fundamental Discoveries in Heterogeneous Catalysis Focus Topic

Room B113 - Session HC+SS-ThA

Closing in on Reality & HC Discovery Reception

Moderators: Liney Arnadottir, Oregon State University, Ashleigh Baber, James Madison University, Dan Killelea, Loyola University Chicago

2:20pm **HC+SS-ThA-1 Ion Imaging applied to Heterogeneous Catalysis on Metals, Theofanis Kitsopoulos**, University of Southern Mississippi **INVITED**
I will discuss how to impalement ion imaging methods to measure the kinetics and dynamics of elementary reaction on metal surfaces. I will discuss the recombination of H atoms on Pt and Pd, followed by a discussion on the kinetics of formic acid adsorption on Pt and Pd

3:00pm **HC+SS-ThA-3 Structure-Sensitive Metal-Support Interactions – Applications to Selective Hydrogenation Reactions, Helena Hagelin Weaver, H. Zhao, M. Lapak, L. Hsiao, D. Choi, C. Bowers**, University of Florida **INVITED**

Producing hyperpolarized molecules is important for increasing signal intensities in nuclear magnetic resonance (NMR) or magnetic resonance imaging (MRI) applications, and one efficient strategy is to add a parahydrogen molecule, where the nuclei have antiparallel spins, to an unsaturated substrate. The requirements for the production of a hyperpolarized molecule are that the added hydrogens must come from the same hydrogen molecule, i.e. a pairwise addition, the spins must be preserved, and the hydrogens in the generated product must be inequivalent. While this is efficient over homogeneous organometallic catalysts, heterogeneous catalysts would be preferred to facilitate separation of hyperpolarized product from the catalyst and allow continuous operation. However, over typical heterogeneous catalysts, i.e. oxide-supported metal nanoparticles, the pairwise addition of parahydrogen is challenging due to facile and reversible dissociation of dihydrogen, rapid diffusion of hydrogen atoms across the metal surface, step-wise addition of hydrogen atoms to the unsaturated molecule, and spillover of hydrogen from the active metal to the oxide support, as these are all mechanisms that can lead to a rapid loss in the singlet spin-correlation of the original parahydrogen molecule. Therefore, the pairwise selectivity in hydrogenation reactions over supported metal catalysts is often very low (< 1%).

To limit diffusion of hydrogen across the metal surface and improve the pairwise selectivity in the hydrogenation of propene, the metal particle size was first reduced to the limit, i.e. single atoms on the support. Single atoms on an oxide support are indeed more selective to pairwise addition of parahydrogen than larger nanoparticles of the same metal, but the activity is low and stability is an issue during reaction conditions. Another approach is to limit diffusion by blocking metal sites with an oxide overlayer. This was done by inducing strong metal-support interactions via a high-temperature reduction of titania-supported catalysts. The structure of the titania support, anatase versus rutile, influenced the metal-support interactions, and active metals, such as Rh and Ir, exhibited different behavior in the pairwise selective addition of parahydrogen to propene. However, in all cases, the high temperature reduction increased the pairwise selectivity regardless of whether geometric (migration of titania over metal) or electronic metal-support interactions were induced. Preliminary data reveal that oxide layers deposited by ALD can also improve the pairwise selectivity in hydrogenation reactions.

3:40pm **HC+SS-ThA-5 High Activity and Selectivity of Dilute Ti-Cu(111) Alloys Toward the Deoxygenation of Ethanol to Ethylene, J. Shi**, University of Florida; **H. Ngan, P. Sautet**, University of California at Los Angeles; **Jason Weaver**, University of Florida

Alloys comprised of an early transition metal dispersed in a coinage metal can provide opportunities for effecting selective chemical transformations of organic oxygenates and other compounds. In this talk, I will discuss our recent work to synthesize dilute Ti-Cu(111) surface alloys in ultrahigh vacuum and characterize their structural and chemical properties using experiments and DFT. We find that Cu-capped, Ti-containing islands are preferentially generated on step edges of Cu(111) during Ti deposition below ~500 K, whereas Ti atoms alloy into the step edges during deposition above 500 K. These dilute Ti-Cu(111) surfaces are highly selective for the deoxygenation of ethanol, resulting in the production of only C₂H₄ and H₂ near 400 K during temperature programmed reaction spectroscopy. DFT

calculations corroborate the high selectivity of metallic Ti-Cu(111) surfaces toward ethanol deoxygenation and predict that C₂H₄ production becomes significantly favored as the Ti ensemble size is increased from monomer to trimer, and that the O released to Ti during C-O bond cleavage promotes desorption of the C₂H₄ product by destabilizing its adsorbed state.

Surface Science Division

Room D136 - Session SS+HC-ThA

Alloys and Complex Surfaces

Moderators: Arthur Utz, Tufts University, Zhenrong Zhang, Baylor University

2:20pm **SS+HC-ThA-1 Single-Atom Alloy Catalysts: Born in a Vacuum, Tested in Reactors, and Understood In Silico, E Charles Sykes**, Tufts University **INVITED**

In this talk I will discuss a new class of heterogeneous catalysts called *Single-Atom Alloys* in which precious, reactive metals are utilized at the ultimate limit of efficiency. These catalysts were discovered by combining atomic-scale scanning probes with more traditional approaches to study surface-catalyzed chemical reactions. This research provided links between atomic-scale surface structure and reactivity which are key to understanding and ultimately controlling important catalytic processes. In collaboration with Maria Flytzani-Stephanopoulos these concepts derived from our surface science and theoretical calculations have been used to design *Single-Atom Alloy* nanoparticle catalysts that are shown to perform industrially relevant reactions at realistic reaction conditions. For example, alloying elements like platinum and palladium with cheaper, less reactive host metals like copper enables 1) dramatic cost savings in catalyst manufacture, 2) more selective hydrogenation and dehydrogenation reactions, 3) reduced susceptibility to CO poisoning, and 4) higher resistance to deactivation by coking. I go on to describe very recent theory work by collaborators Stamatakis (UCL) and Michaelides (Cambridge University) that predicts reactivity trends for a wide range of *Single-Atom Alloy* combinations for important reaction steps like H-H, C-H, N-H, O-H, and CO₂ activation. Overall, I hope to highlight that this combined surface science, theoretical, and catalyst synthesis and testing approach provides a new and somewhat general method for the a priori design of new heterogeneous catalysts.

3:00pm **SS+HC-ThA-3 Heterogeneities in Early Oxide Evolution on Ni-Cr Alloys Studied with a Combination of XPEEM and Data Analytics Methods, Keithen Orson**, University of Virginia; **W. Blades**, University of Arizona; **Y. Niu, A. Zakharov**, Max IV Laboratory, Sweden; **P. Reinke**, University of Virginia

The Ni-Cr alloy system is coveted for its mechanical properties and its resistance to degradation in high-temperature, corrosive environments. This resistance comes primarily from a chemically complex passive film composed of nanometers-thin layer of oxides and hydroxides, but many questions remain about the early stages of passive film growth. Studying this early regime gives insights into how surface orientation and features like grain boundary influence oxide nucleation and growth. The early regime is also where competition between Ni and Cr oxidation occurs on the surface. We studied oxide growth on Ni_{22wt%Cr} using the XPEEM techniques μ -XAS and μ -XPS, giving chemical specificity with a pixel size of 50 nm. We conducted a controlled oxidation on a clean surface with up to 65 L of oxygen at 773 K which records oxide evolution with video rate focused on a region with (212) and (104) surfaces and the corresponding grain boundary. To address the size and complexity of the hyperspectral images we use Principal Component Analysis (PCA) and Non-Negative Matrix Analysis (NNMA) to identify the various spectral components and thus bonding states in the image with spatial and temporal resolution. The Ni L-edge spectra change little over the oxidation process and are characteristic for Ni(O) in line with the known preponderance of Cr oxidation under these conditions. All XAS images include image artifacts mostly seen as modulation of background intensity and slope. Valence band spectra (h ν =95 eV) reveal grain-dependent work function shifts and appear characteristic of the bonding state for O_{ads}. The Cr L-edge shows strong spatial heterogeneities, with NNMA revealing the emergence of chromia nuclei. PCA, while less directly interpretable, gives good qualitative agreement with the NNMA. NNMA analysis informs segmentation of movies taken at a single energy in the Cr-L edge characteristic of oxide. Island nucleation begins between 5 and 20 L of exposure and a logistic growth behavior up to 65L of exposure consistent with Avrami-type nucleation. Chromium oxide particle density and distribution varies widely

Thursday Afternoon, November 9, 2023

across the two grains, while particle size remains nearly constant. 21% of the (212) grain is covered evenly by oxide particles, while particle density on (104) is only 11% at the endpoint of the oxidation experiment. A region in the vicinity of the grain boundary on (212) is nearly devoid of chromia particles. In summary, early-stage Ni-Cr oxidation is grain- and texture-specific with chromia island growth dominating in the 0-65 L oxidation regime. Work function shifts and O adsorbates possibly play a role in these heterogeneities behavior.

3:20pm **SS+HC-ThA-4 The Impact of Crystallographic Orientation on the Oxidation of Ni-Cr Alloys**, *Petra Reinke*, University of Virginia, USA; *W. Blades*, Arizona State University; *D. Jessup*, *J. St.Martin*, *K. Orson*, University of Virginia, USA

Ni-Cr alloys in the FCC random solid solution structure are coveted for their mechanical properties combined with a superb corrosion resistance and thermal stability. The corrosion resistance in aqueous solution, specifically pitting resistance, can be further improved by addition of a third alloying element such as Mo or W. [1] The role of alloy composition and temperature is well studied but significant knowledge gaps exist in our understanding of the initial oxidation steps until complete oxide layers have formed and Cabrera-Mott type growth models can be applied. The competition between Ni and Cr oxidation plays out at < 873 K of relevance for many energy applications. This regime is highly sensitive to the specifics of surface reactions but also impacted by alloy microstructure. The crystallographic orientation of the surface varies significantly between adjacent grains, and reaches deep into the crystallographic triangle with complex terrace and kink structures. Ni-Cr(100) and Ni-Cr(111) surfaces show highly distinct oxidation pathways modulated by the interfacial epitaxy between NiO and the alloy surface. [2,3] Recent work demonstrated that the pitting resistance in acidic solution is strongly grain orientation dependent. [4] It can be assumed that the orientation of oxide grains in the protective layer leads to contact potentials which influence reactant and vacancy diffusion across the oxide layer as the growth continues.

We will present combined STM, in-situ and operando XPS studies which resolve the oxidation process as a function of crystallographic orientation. We will introduce our approach to identify, and study individual grains with wide variability in surface (h k l) through a combination of metallurgical processing, EBSD, and SEM. The oxidation of individual grains is then be studied and significant variation in oxidation rate and oxide composition are isolated. Thermally induced faceting adds to the complexity of orientation dependent oxidation. It is generally assumed that the epitaxial relation between Ni-Cr and NiO drives its rapid nucleation and layered growth mode. We are extending this assessment beyond the well-studied singular surfaces and calculate structural interfacial models which will also include several chromia surfaces albeit chromia tends to nucleate as sub-oxide surface clusters. [2] The role of interfacial energies in the initial oxidation steps will be assessed for the singular and higher index surfaces.

[1] C. Volders *et al.* *npj Materials Degradation* **6**, 52 (2022).

[2] W. H. Blades *et al.* *ACS Applied Materials & Interfaces* **10**, 43219-43229 (2018).

[3] W. H. Blades *et al.* *Corrosion Science* **209**, 110755 (2022).

[4] K. Gusieva *et al.* *The Journal of Physical Chemistry C* **122**, 19499-19513 (2018).

3:40pm **SS+HC-ThA-5 Structure of Electrochemical Electrode/Electrolyte Interfaces from First Principles**, *Axel Groß*, University of Ulm, Germany

Our knowledge about structures and processes at electrochemical electrode-electrolyte interfaces is still rather limited, in spite of its technological relevance in energy conversion and storage. First-principles simulations can help to elucidate these structures in spite of the fact that these simulations are hampered by the complexity of these interfaces together with the fact that the dependence of these interfaces on the electrode potential needs to be properly taken into account. In this contribution, I will first show which insights first-principles calculations can provide with respect to halide and sulfate adsorbate structures at electrochemical interfaces [1,2] using grand-canonical approaches yielding reliable Pourbaix diagrams of the stable adsorbate phases. Furthermore I will demonstrate how ab initio molecular dynamics simulations can contribute to a better understanding of the structure of electric double layers at metal electrodes [3,4]. The presentation will conclude with some general remarks about remaining challenges in our understanding of electrochemical electrolyte/electrode interfaces [5].

References

- [1] F. Gossenberger, F. Juarez, and A. Groß, *Front. Chem.* **8**, 634 (2020).
- [2] A. Groß, *J. Phys. Chem. C* **126**, 11439 (2022).
- [3] S. Sakong and Axel Groß, *Phys. Chem. Chem. Phys.* **22**, 10431 (2020).
- [4] A. Groß and S. Sakong, *Chem. Rev.* **122**, 10746-10776 (2022).
- [5] A. Groß, *Curr. Opin. Electrochem.* **40**, 101345 (2023).

4:00pm **SS+HC-ThA-6 Surface Characteristics of Flexible Carbon-Doped Oxide Thin Films Under Reactive Ion Etching Process Using Fluorocarbon-Based Plasma**, *Seonhee Jang*, *T. Poche*, *R. Chowdhury*, University of Louisiana at Lafayette

The microelectronics industry is increasing research on flexible electronics. Instead of the traditional rigid Si-based electronics, flexible electronics utilize polymer substrates that allow stretching, bending, and folding of the device, which drastically expand its applications. A wide variety of inorganic materials, semiconductors, dielectrics, and metals have been integrated for the fabrication of flexible electronic devices. One of the dielectric materials employed in semiconductor devices is carbon-doped silicon oxide (SiCOH). In this study, flexible low-k SiCOH films were produced by plasma-enhanced chemical vapor deposition (PECVD) of tetrakis(trimethylsilyloxy)silane (C₁₂H₃₆O₄Si₅) precursor onto flexible indium tin oxide/polyethylene naphthalate (ITO/PEN) substrates using a set of different plasma powers, yielding the films with varying material properties. The physical properties including refractive index, extinction coefficient, surface morphology and roughness, and surface wettability were determined. The surface structures were analyzed by Fourier transform infrared (FTIR) and X-ray photoelectron (XPS) spectra. Four prominent peaks of Si-O-Si stretching, Si-CH₃ bending, Si-(CH₃)_x stretching, and CH_x stretching modes were observed in the FTIR spectra. High-resolution XPS spectra of Si2p, C1s, and F1s were analyzed for the chemical bond structure and elemental composition. Mechanical properties including elastic modulus and hardness were measured using nanoindentation. The pristine SiCOH films were then subjected to an inductively coupled plasma-reactive ion etching (ICP-RIE) process. The etching properties of the flexible SiCOH films were characterized under a set of fluorocarbon (CF₄)-based plasmas such as CF₄, CF₄+O₂, and CF₄+Ar. The CF₄ flow rate was maintained at 35 sccm while the O₂ and Ar flow rates were both at 24 sccm. The RF plasma at 13.56 MHz was maintained at 200 W and the ICP power at 40 W. The operating pressure and temperature were 10.0 Pa and ambient temperature, respectively. The duration for etching process was 30 s. Using deconvolution of FTIR and XPS spectra, the surface structures of the SiCOH films after etching process were compared with those of the pristine film. The fraction ratios of the deconvoluted peaks in each prominent peak in the FTIR spectra depended on the deposition plasma power and RIE etching gas composition. In the XPS spectra analysis, each Si2p and C1s peak showed a depressed peak intensity after etching process. With additional etchants of O₂ and Ar, the F1s peak shifted to higher binding energy for lower deposition plasma power and lower binding energy for higher deposition plasma power. Surface properties of flexible SiCOH films after etching were changed according to composition of etchants.

Fundamental Discoveries in Heterogeneous Catalysis Focus Topic

Room Oregon Ballroom 203-204 - Session HC-ThP

Fundamental Discoveries in Heterogeneous Catalysis Poster Session

HC-ThP-1 Insight into Synergistic Effect of Oxide-Metal Interface on Hot Electron Excitation, Eunji Lee, Korea National University of Education, Republic of Korea; B. Jeon, J. Park, Korea Advanced Institute of Science and Technology (KAIST), Republic of Korea; S. Lee, Korea National University of Education, Republic of Korea

Understanding the role of electron transfer by energy dissipation during chemical reactions on metal catalyst surfaces is significant for elucidating the fundamental phenomena at solid-gas and solid-liquid interfaces [1]. Electronic excitation by molecular interactions between reactants and catalyst surfaces generates a flow of excited electrons with an energy of 1–3 eV; these are called hot electrons [2]. To reveal the chemically induced electronic excitations on metal catalyst surfaces, metal-semiconductor catalytic nanodiodes can be used for real-time hot electron detector [3]. In addition, recently, it was found that when the metal-oxide interface is formed, the excitation of hot electrons can be amplified [4].

In this work, to understand the effect of the oxide-metal interface on hot electron excitation under exothermic chemical reactions, we employ advanced real-time detection of reaction-induced electronic excitation and report, for the first time, direct *in-situ* observations of hot electron transfer on metal-semiconductor Schottky nanodevices with well-controlled oxide-metal interfaces (CeO₂ nanocubes/Pt/TiO₂ Schottky nanodiodes). Direct measurement of the electron transfer according to the concentration of interfacial sites (by controlling the coverages of deposited CeO₂ on Pt) allows us to investigate the effect of the oxide-metal interface on non-adiabatic electronic excitation during catalytic H₂ oxidation. Surprisingly, when compared according to the concentration of the CeO₂/Pt interface, the efficiency of hot electron excitation appears to be the highest at a specific concentration of interfacial sites, proving that the inverse oxide-metal interface plays an important role in improving hot electron excitation under exothermic catalytic reactions. Our *operando* techniques using Schottky nanodiodes with well-controlled oxide-metal interfaces provide conclusive evidence about the promotional role of the inverse oxide-metal interfacial sites in heterogeneous catalysts, which contributes to the rational design of future hot electron-based catalysts [5].

References

- [1] Jeong Young Park* *et al.*, *Chemical Reviews*, **2015**, 115 (8), 2781
- [2] Si Woo Lee *et al.*, *Surface Science Reports*, **2021**, 76 (3), 100532
- [3] Si Woo Lee *et al.*, *ACS Catalysis*, **2019**, 9 (9), 8424
- [4] Si Woo Lee *et al.*, *Nature Communications*, **2021**, 12 (40), 1
- [5] Eunji Lee *et al.*, *in preparation*

HC-ThP-2 Chemical Speciation and Structural Evolution of Rhodium and Silver Surfaces with High Oxygen Coverages, Dan Killelea, M. Turano, L. Jamka, M. Gillum, Loyola University Chicago; L. Juurlink, Leiden University, The Netherlands; T. Schäfer, University of Göttingen, Germany

The oxidation silver and rhodium surfaces are compared. In particular, I will discuss how the structures formed at high oxygen coverages differ for the metals and how their chemistries may be affected.

The interaction of oxygen with the surfaces of catalytically active transition metals has attracted much interest because of the relevance to heterogeneous catalysis. Recently, we have shown that oxygen coverages in excess of 1 ML are achievable using gas-phase atomic oxygen (AO) to dose the metal surfaces. This talk will discuss some recent results comparing the uptake of AO and O₂ on Ag(111), Rh(111), and curved Ag(111). On c-Ag(111) surfaces, the geometry of the monoatomic steps determines whether or not O will accumulate and the consequent surface

reconstruction. Conversely, on Rh(111), subsurface oxygen readily forms from exposure to AO. Finally, the uptake of oxygen on Ag(111) is discussed; unlike Rh(111), where little surface reconstruction occurs, Ag(111) undergoes several phase transformations as the oxygen coverage is increased. These results using AO demonstrate that UHV compatible dosing can prepare the same surfaces resulting high pressure O₂ exposures, allowing for quantitative and structural analysis of the oxidized surfaces.

HC-ThP-3 Exploring Field-Assisted Nitrogen Activation with Atom Probe Microscopy, Sten V Lambeets, M. Wirth, D. Perea, Pacific Northwest National Laboratory

Challenges in the development of green electricity and energy storage challenges are leading us to consider NH₃ as a promising future zero-carbon fuel. However, NH₃ production largely relies on the Haber-Bosch process requiring high temperature and pressure, making its production via this means responsible for approximately 1.5% of world CO₂ emissions. To unlock to full economic and environmental potential of NH₃, it is critical to lower energy requirements and generate a zero-carbon NH₃ by coupling with renewable electricity¹. The N₂ reduction reaction to NH₃ using electricity is extensively investigated with single atom electrocatalysts (SACs) recently showing promising results. Due to their morphology, the application of an electrical potential on SACs materials results in local High External Electric Fields (HEEFs) over the single atoms. If those effects present promising outcomes according to theoretical calculations^{2,3}, the values of those HEEFs and the mechanisms involved remains largely unknown and unexplored.

Atom Probe Microscopy (APM) such as Field Ion Microscopy (FIM) and Operando Atom Probe (OAP) are ideal techniques to unravel those mechanisms at the nanoscale since they inherently rely on HEEFs for imaging. In this work, we will illustrate those capabilities with the room temperature N₂ dissociation over Ru single nanoparticle case imaged at the nanoscale using FIM and OAP.

We use the recently developed OAP technique⁴ to effectively measure this dissociation over a 0001-oriented Ru specimen. After fixing a constant HEEF between 15 and 25 V/nm and the temperature at 300K, 1.4x10⁻⁷mbar N₂ pure gas is introduced in the analytic chamber. The electric field either directly ionize N₂ or provoke its dissociation. Dissociated N(ads) are mainly detected over the Ru{1012} facets while ionized N₂⁺⁺ are detected on large areas in the periphery of the imaged apex. The occurrence of one or the other processes is intimately linked to the local surface structures and, subsequently, the local HEEFs.

APM are capable to observe and estimate the HEEF necessary to trigger specific chemical reaction steps such as the N₂ dissociative adsorption (i.e. activation). With an accurate calculation of those HEEF, those values can be extrapolated to create new chemical and reactor system designed to perform N₂ activation at relatively low energy cost. In a context of electrification of chemical processes, APM can help pave the way to a deeper understanding of the physical laws involved in electrochemistry, as well as in chemistry in general.

- 1.M.Wan *et al.* *JACS* Au 2,1338–1349(2022).
- 2.S.M.Kathmann, *Phys.Chem.Chem.Phys.*23,23836–23849(2021).
- 3.M.L.Karahka&H.J.Kreuzer, *Surf.Sci.*643,164–171(2016).
- 4.S.V.Lambeets *et al.* *Top.Catal.*1606-1622(2020)

HC-ThP-4 Adsorption and Hydrogenation of 1,3-Butadiene on Cu (111) and a Pd/Cu (111) Single-Atom-Alloy, Mohammad Rahat Hossain, M. Trenary, University of Illinois - Chicago

A single atom alloy (SAA) is made by substituting catalytically active dopant metal atoms into the topmost atomic layer of a relatively inert host metal. Commonly, Pd and Pt are used for hydrogenation reactions due to their virtually zero barrier for H₂ activation. Yet, these catalysts are easily coked by CO and their high activity often limits their selectivity. Industrially, these catalysts are often doped with a less active metal to prevent coking and enhance their selectivity. One of the most important steps in the refinement of alkene streams for the industrial-scale production of high-quality polymers is the selective hydrogenation of 1,3-butadiene. In the literature, Pd (111) shows higher selective control over hydrogenation of 1,3-butadiene to butene than Pt (111). Therefore, the presence of isolated

Pd atoms on a Cu host surface can be a suitable SAA catalyst model for this particular reaction. In this study, we used reflection absorption infrared spectroscopy (RAIRS) and temperature programmed desorption (TPD) to investigate the adsorption of butadiene and butene, as well as the hydrogenation of butadiene on Cu (111) and a Pd/Cu (111) SAA. The TPD study shows butadiene binds strongly to the Cu (111) surface compared to 1-butene. The desorption peak in the 120-130 K temperature range indicates the production of 1-butene from the hydrogenation of butadiene on the Pd/Cu (111) SAA. Auger electron spectroscopy (AES) shows no accumulation of surface carbon demonstrating molecular desorption of butadiene from the surface under UHV. The observation of both in-plane (CH_2 -wag at 908 cm^{-1}) and out-of-plane (C-H bend at 1023 cm^{-1}) modes with RAIRS at monolayer coverage indicates that butadiene is adsorbed neither parallel nor perpendicular to the surface. In addition, IR peaks at 1464 cm^{-1} for ($-\text{CH}_3$) antisymmetric deformation and 1412 cm^{-1} for ($=\text{CH}_2$) scissors modes are observed on the Pd/Cu (111) SAA, indicating 1-butene formation from butadiene hydrogenation. The ambient pressure RAIRS studies are currently underway to calculate the turnover frequency (TOF) of the above-mentioned catalyst for the hydrogenation of 1,3-butadiene.

HC-ThP-5 Studying C-H Activation on RhCu Single-Atom Alloys Using Molecular Beams, Molly Powers, J. Rosenstein, L. Joseph, A. Utz, Tufts University

Single-atom alloys (SAAs) are a new class of heterogeneous catalysts drawing immense research interest due to their unique catalytic activity. An active dopant metal is atomically dispersed in a more inert, selective host metal to produce a catalyst that has a unique potential to simultaneously improve catalytic selectivity and activity compared to their single metal counterparts. To date, detailed surface science studies of SAAs have been limited to relatively low-barrier reactions. The poster will summarize recent work in our lab that extends the range of detailed mechanistic studies to higher barrier reactions, including C-H activation. Our study focuses on the reaction of simple hydrocarbons, such as methane, on a RhCu SAA catalyst. While prior work has examined this system using reflection-absorption IR spectroscopy, temperature programmed desorption, and scanning tunneling microscopy, our supersonic molecular beam experiments permit the study of high energetic barriers to examine the dynamics, kinetics, and energetics of the initial C-H bond cleavage reaction, and the subsequent chemistry and diffusion of the surface-bound products of dissociative chemisorption.

HC-ThP-6 Investigating the Dissociative Chemisorption of Methane on Ru(0001) via Supersonic Molecular Beam, Matthew Kalan, Y. Li, A. Utz, Tufts University

Recent theoretical studies have proposed the creation of a database of experimentally determined barrier heights for model reactions on transition metal surfaces as a tool for the development of chemically accurate computational methods for heterogeneously catalyzed reactions¹. This approach has been effectively applied to the dissociative chemisorption of CH_4 on Pt and Ni surfaces using semi-empirical specific reaction parameter density functional theory (SRP-DFT)². Current work on SRP-DFT involves expanding its application to other surfaces, including Ru(0001). There is, however, substantial disagreement in the current literature as to the height of the barrier on Ru(0001), with experimentally determined values ranging from 0.38 to 0.85^{3,4} eV. Our work applies supersonic molecular beam reactivity measurements to this system in order to provide an important experimental benchmark for additional SRP-DFT studies. By measuring reactivity across a wide range of translational energies, surface temperatures, and vibrational states, our data will also serve as a rigorous test of the theoretical predictions of any future first-principles methods. We will present the results from ongoing reactivity measurements of the dissociative chemisorption of CH_4 on Ru(0001) and their implications for the dynamics of the reaction.

(1) Mallikarjun Sharada, S.; Bligaard, T.; Luntz, A. C.; Kroes, G.-J.; Nørskov, J. K. SBH10: A Benchmark Database of Barrier Heights on Transition Metal Surfaces. *J. Phys. Chem. C* **2017**, *121* (36), 19807–19815. <https://doi.org/10.1021/acs.jpcc.7b05677>.

(2) Migliorini, D.; Chadwick, H.; Nattino, F.; Gutiérrez-González, A.; Dombrowski, E.; High, E. A.; Guo, H.; Utz, A. L.; Jackson, B.; Beck, R. D.; Kroes, G.-J. Surface Reaction Barriometry: Methane Dissociation on Flat and Stepped Transition-Metal Surfaces. *J. Phys. Chem. Lett.* **2017**, *8* (17), 4177–4182. <https://doi.org/10.1021/acs.jpclett.7b01905>.

(3) Larsen, J. H.; Holmblad, P. M.; Chorkendorff, I. Dissociative Sticking of CH_4 on Ru(0001). *7*.

(4) Mortensen, H.; Diekhöner, L.; Baurichter, A.; Luntz, A. C. CH_4 Dissociation on Ru(0001): A View from Both Sides of the Barrier. *The Journal of Chemical Physics* **2002**, *116* (13), 5781–5794. <https://doi.org/10.1063/1.1456509>.

HC-ThP-7 Size-Selected Pt Alloy Cluster Catalysts for the Dehydrogenation of Light Alkanes, Autumn Fuchs, M. Malek, S. Anderson, University of Utah

Size-selected Pt_nGe_m clusters supported on alumina have been developed and are being investigated under ultra-high vacuum for the selective dehydrogenation of light alkanes. Surface analysis techniques such as temperature programmed desorption (TPD), x-ray photoelectron spectroscopy (XPS), and ion scattering spectroscopy (ISS), are used to characterize the clusters and probe binding sites and energies of small alkanes. TPD experiments have shown that the addition of Ge to Pt_n limits catalyst deactivation by carbon deposition (coking) and sintering. The number of Pt atoms in the cluster affects the number of available binding sites for ethylene on the surface. We will present a study of butane and isobutane dehydrogenation and cracking $\text{Pt}_n/\text{alumina}$ and $\text{Pt}_n/\text{Ge}_m/\text{alumina}$. In addition to the surface science experiments, we will present data from a MEMS microreactor device that allows reactants to be flowed over a sample of deposited clusters at pressures up to 1 atm and temperatures to 1000 K. Reactions on clusters will be compared to reactions on Pt nanoparticles made via chloroplatinate drop-casting and reduction.

HC-ThP-8 Switching between Hot Electron and Hot Hole Transfer during Chemical Reaction, Hyekyung Kwon, Korea National University of Education, Republic of Korea; B. Jeon, J. Park, Korea Advanced Institute of Science and Technology (KAIST), Republic of Korea; S. Lee, Korea National University of Education, Republic of Korea

Understanding hot carrier dynamics is crucial for the rapid development of nanocatalysts [1]. By observing the transfer of carriers quantitatively in real-time during a catalytic reaction, a correlation between catalytic performance and charge transfer can be identified [2]. When a chemical reaction occurs on a metal catalyst, electronic excitation is caused by the non-adiabatic dissipation of exothermic energy, leading to the generation of electron-hole pairs (*i.e.*, hot carriers) [3]. In order to study the surface dynamics of these hot carriers, a metal/semiconductor Schottky (*i.e.*, catalytic nanodiode) needs to be coupled with heterogeneous catalysts [4].

In this work, we observed hot carriers excited in real time during the H_2O_2 decomposition reaction using Pt/Si Schottky nanodiodes. When the Pt/Si nanodiode was immersed in the H_2O_2 solution, the H_2O_2 decomposition occurred on the Pt catalyst surface, and electron-hole pairs were excited. This could be detected as a current signal (*i.e.*, chemicurrent; a current induced by a chemical reaction) flowing through the nanodevice. Interestingly, the flow of hot electrons was detected in the Pt/n-Si nanodiode, whereas the transfer of hot holes was observed in the Pt/p-Si nanodiode. The chemicurrent caused by hot carrier transfer linearly depended on the concentration of the H_2O_2 solution, confirming that the observed chemicurrent was indeed a result of the H_2O_2 decomposition occurring on the Pt catalyst. In order to electronically control the hot electron and hot hole transfers, we detected the currents while applying a reverse bias (*i.e.*, an electric field on the Schottky junction) to both the Pt/n-Si and Pt/p-Si nanodevices. In the Pt/n-Si nanodiode, through which hot electrons flowed, electron transfer was amplified under the reverse bias condition due to Schottky barrier lowering. However, when reverse bias was applied to the Pt/p-Si nanodevice, where hot hole transfer was dominant under open circuit, hot electron transfer surprisingly emerged instead of hot hole transfer. Accordingly, we can conclude that the movement of the hot hole in the Pt/p-Si nanodiode was due to the remaining holes after the electrons were consumed for inducing the chemical reaction. Our techniques to control and switch the transfer of hot carriers during a chemical reaction using metal-semiconductor Schottky junctions may shed light on potential applications of hot carriers in catalytic devices, energy conversion-based devices, or sensors.

References

[1] Si Woo Lee *et al.*, *Surface Science Reports*, **2021**, *76* (3), 100532

[2] Si Woo Lee *et al.*, *ACS Catalysis*, **2019**, *9* (9), 8424

[3] Si Woo Lee *et al.*, *Nano Letters*, **2023**, *23* (11), 5373

[4] Si Woo Lee *et al.*, *Nature Communications*, **2021**, *12* (40), 1

Thursday Evening, November 9, 2023

HC-ThP-9 Tracking Elementary Steps in Conversion of Carboxylic Acids on Single Crystalline and Nanofaceted TiO₂(101), Xingyu Wang, Pacific Northwest National Laboratory; *W. Debenedetti,* Los Alamos National Laboratory; *C. O'Connor,* Harvard University; *Z. Dohnalek, G. Kimmel,* Pacific Northwest National Laboratory

In catalysis research, the material gap is one of several that the surface science community is trying to bridge, along with the pressure and temperature gaps. In the specific case of carboxylic acids on TiO₂, previous studies discovered that for acetic acid reacting with anatase nanoparticles at ambient pressure, an environment very much like real world catalytic processes, acetone could be produced. However, under ultrahigh vacuum (UHV) conditions, with a few monolayers of acetic acid on anatase(101) single crystals, acetone was not observed as a product. In contrast, formic acid reactions with either nanoparticles or single crystals showed no evidence of C-C bond formation. Here, we prepared a sample with layers of synthesized anatase nanoparticles with mostly (101) facets in an UHV system and compared the reactivity of acetic acid with that on an anatase(101) single crystal, using TPD (temperature programmed desorption) and RAIRS (reflection absorption infrared spectroscopy) to track the elementary steps, with the goal to bridge this material gap and fully understand the reaction mechanisms of carboxylic acids on metal oxides.

HC-ThP-10 ZnO Nanoparticles as an Effective Rhodamine B Dye Mineralization Under Direct Sunlight Irradiation, Jose Alberto Alvarado Garcia, BENEMERITA UNIVERSIDAD AUTONOMA DE PUEBLA, Mexico; *G. ANAYA GONZALEZ,* Universidad Autónoma de Mexico; *R. PEREZ CUAPIO, H. JUAREZ SANTIESTEBAN,* BENEMERITA UNIVERSIDAD AUTONOMA DE PUEBLA, Mexico; *A. ARCE PLAZA,* INSTITUTO POLITÉCNICO NACIONAL, Mexico

In this research ZnO at different Zinc acetate concentration from 0.1-0.4 M was synthesized through colloidal synthesis and applied to mineralize Rhodamine B dye under direct sunlight irradiation, showing that this is strongly related to the particle size and defects presence at the particle. This relationship is well correlated to the UV-Vis absorbance spectrum and photoluminescence (PL), showing up to 90 % of photocatalyst efficiency after 100 min for sample obtained at 0.3M, this behavior also is showed for those samples obtained at 0.1, 0.2 and 0.4 molar concentration. The XRD data analysis let the structure and crystallite average size (18- 27 nm) to be determined meanwhile the morphology and composition was obtained from HRSEM and EDS respectively. From the FTIR results the organic dye mineralization evolution was determined. Albeit the defects contribution was determined by PL.

HC-ThP-11 Role of Vacancies and Absorbed Hydrogen Atoms on the Formation of Peroxides and Superoxides on CeO₂ Surfaces, M. Brites Helu, M. Vecchiotti, S. Collins, Instituto de Desarrollo Tecnológico para la Industria Química, Argentina; *M. Calatayud,* Laboratoire de Chimie Théorique, Sorbonne Université, France; *Jorge Anibal Boscoboinik, D. Stacchiola,* Center for Functional Nanomaterials, Brookhaven National Laboratory; *F. Calaza,* Instituto de Desarrollo Tecnológico para la Industria Química, Argentina

It is well known that VOCs being recognized as major responsible for the increase in global air pollution. Catalytic combustion is an efficient technology for the abatement of VOC, which are oxidized over a catalyst at temperatures much lower than those of the thermal process. Specifically, gold supported catalysts on CeO₂ have shown a great performance in the oxidation of CO, methanol, toluene, etc. Besides, it is important to clarify the role of the support in such reaction. Ceria has the key property of high oxygen storage capacity which originates in its ability to rapidly switch from Ce to Ce oxidation states as the environment changes from reducing to oxidizing and vice versa. Its redox behavior is influenced by the substituent lattice groups that could be incorporated during different catalyst pretreatments and could affect the oxidation of VOC. This could be understood as the influence of oxygen vacancies and/or absorbed or coadsorbed H on the activation of oxygen molecules. The latter leads to the formation of superoxide and peroxide molecules on the surface, which could in principle be highly reactive towards oxidation of organic molecules.

In this context, we study, by IR spectroscopy and mass spectrometry, the interaction of O₂ with the modified CeO₂ based material, by creating vacancies following different reduction treatments. The possible role of the vacancies and/or presence of H atoms in the electron transfer from the surface to the oxygen molecule is discussed. Using AP-XPS we are able to prove that the surface/near surface of CeOx presents a charging effect which could be due to extra charge/electrons which then transfer to O₂ to form superoxide and peroxide species sequentially and presenting different

thermal stabilities. Furthermore, the presence of different facets on the surface of the material could change the stability or amount of active species, thus comparison of results from polycrystalline ceria and CeO₂ nanocubes provide information about the structure-activity relationship for the rational design of catalytic materials.

HC-ThP-12 Small Alcohol Reactivity Over TiO₂/Au(111) Inverse Model Catalysts, Ashleigh Baber, James Madison University

Gold-based catalysts have received tremendous attention as supports and nanoparticles for heterogeneous catalysis, in part due to the ability of nanoscale Au to catalyze reactions at low temperatures in oxidative environments. Surface defects are known active sites for low temperature Au chemistry, so a full understanding of the interplay between intermolecular interactions and surface morphology is essential to an advanced understanding of catalytic behavior and efficiency. Our undergraduate research lab uses ultrahigh vacuum temperature programmed desorption (UHV-TPD) to investigate the fundamental interactions between small alcohols on Au(111) and the reactivity of TiO₂/Au(111) inverse model catalysts on small alcohol redox behavior. In a systematic study to better understand the adsorption and intermolecular behavior of small alcohols (C₁-C₄) on Au(111) defect sites, coverage studies of methanol, ethanol, 1-propanol, 1-butanol, 2-butanol, and isobutanol have been conducted on Au(111). These small alcohols molecularly adsorb on the Au(111) surface and high resolution experiments reveal distinct terrace, step edge, and kink adsorption features for each molecule. The desorption energy of small primary alcohols was shown to trend linearly with increasing C₁-C₄ carbon chain length, indicating that the H-bonded molecular packing of 1-butanol resembles that of methanol, ethanol, and 1-propanol, while isobutanol and 2-butanol deviate from the trend. These energy insights are particularly interesting when studying the redox behavior of small alcohols over TiO₂/Au(111). Depending on the surface preparation conditions, Au(111) supported TiO₂ nanoparticles react with small alcohols to form either reduced and oxidized products. The reactivity of the surface for ethanol oxidation was altered by controlling the oxidation state of TiO_x (x<2) and coverage of TiO₂. Low coverages of fully oxidized TiO₂ nanoparticles on Au(111) are active for the selective oxidation of ethanol to form acetaldehyde, but not all small alcohols behave similarly.

Fundamental Discoveries in Heterogeneous Catalysis Focus Topic

Room B113 - Session HC+SS-FrM

Greatest Hits in Heterogeneous Catalysis

Moderators: Liney Arnadottir, Oregon State University, Ashleigh Baber, James Madison University, Dan Killelea, Loyola University Chicago

8:20am **HC+SS-FrM-1 CO Characterized Pt/Cu(111) Single Atom Alloy (SAA) for the Hydrogenation of Unsaturated Aldehydes, David Molina, M. Trenary, University of Illinois - Chicago**

The use of heterogeneous catalysts is of high importance in a vast number of industrial processes. A promising new type of heterogeneous catalyst known as single atom alloys (SAAs) greatly reduce the amount of precious metal (e.g. Pt, Pd, Rh, Ru) used and have shown enhancements in selectivity, when compared to their pure counterparts, in various types of reactions, including hydrogenation reactions. Hence, it is important to be able to quantify the amount of precious metal on the surface of these catalysts and understand their properties. We have used reflection absorption infrared spectroscopy (RAIRS) and temperature programmed desorption (TPD) of adsorbed CO were used to probe the properties of Pt/Cu(111) surfaces, ranging from a multilayer film of Pt on Cu(111) to 2% Pt/Cu(111). For Pt deposition on Cu(111) at room temperature, the Pt coverage was varied from a multilayer film to 0.23 monolayer (ML). As the Pt coverage decreased, a RAIR C–O stretch peak in the range of 2041–2050 cm^{-1} showed isolated Pt atoms embedded in the Cu(111) surface. Pt islands were identified by a C–O stretch peak in the range of 2058–2067 cm^{-1} , showing CO on top of Pt atoms. These islands also allowed for CO to bind at bridge sites between two Pt atoms and this was supported by the observed C–O stretch peak at 1852 cm^{-1} . Deposition of low coverages of Pt at 380, 450 and 550 K formed SAAs in which surface Pt is only present as isolated atoms that had replaced Cu atoms in the topmost atomic layer, in agreement with previous studies with scanning tunneling microscopy. Adsorption of CO on top of the Pt atoms of the SAAs leads to a C–O stretch in the range of 2041–2046 cm^{-1} . Compared to the SAA formed by Pt deposition at 380 K, deposition at 450 and 550 K led to more dispersed Pt atoms as indicated by the lack of a shift of the C–O stretch peaks, indicating that the distance between CO molecules was not low enough for dipole-dipole coupling shifts to occur. In all cases, the C–O stretch of CO on the Pt atoms of Pt/Cu(111) was significantly redshifted relative to its value on Pt(111), which is a manifestation of how nearby Cu atoms alter the Pt–CO bonding. The well characterized Pt/Cu(111) SAA is currently being used to study the hydrogenation of model unsaturated aldehydes.

8:40am **HC+SS-FrM-2 Efficient Catalyst and Protection Layer of Ni/ α -Al₂O₃ Catalysts for Improved H₂O/CO₂ Reforming Reaction of CH₄ via Atomic Layer Deposition, Dae Woong Kim, H. Jeong, W. Hong, J. Park, S. Oh, J. Jang, Hyundai Motor Company, Republic of Korea**

Recently, production of synthetic gas by combined steam and CO₂ reforming reaction of CH₄ (CSCR) is proposed for dealing with the energy problem. In the CSCR process as methane reforming reaction, the synthesis of steam (H₂O), CH₄, and CO₂ occurs at high temperatures and pressures in the presence of metal catalysts. [1] In general, Ni-based catalysts are attractive materials because of their relatively high activity and low cost as compared to noble metal catalysts. [2] As a support structure, a thermally stable, acid-free and inert α -Al₂O₃ is a well-known material. [3] However, catalytic pellets through mixed powder sintering have low structural strength as well as poor catalytic utilization due to dead nickel volume. Therefore, atomic layer deposition (ALD) is proposed as a reliable and atomic scale-adjustable process for conformally growing NiO on α -Al₂O₃ surface with an exact thickness. In the case of ALD-based catalyst growth, the reaction efficiency can be maximized without a catalyst dead area because the catalyst is formed only on the active surface where the reforming reaction can occur.

In this work, ALD NiO film was grown on α -Al₂O₃ pellet supporter which is followed by reduction annealing for highly active CSCR reforming catalyst with a low Ni concentration. Furthermore, an ultra-thin Al₂O₃ protection layer was proposed to enhance stability and coking resistant of Ni/ α -Al₂O₃ catalyst during reforming reaction. Detailed experimental results will be presented.

[1] Energy Fuels 2015, 29, 1055–1065

[2] RSC Advanced 2015, 5, 7539–7546

[3] Journal of Energy Chemistry 22(2013)919–927

[4] Catalysis Science & Technology 2020, 10, 8283

9:00am **HC+SS-FrM-3 Complementary Outer Atomic Layer Analysis of Catalyst Materials Using LEIS, P. Brüner, IONTOF GmbH, Germany; J. Järvillehto, Department of Chemical and Metallurgical Engineering, Aalto University School of Chemical Engineering, Finland; S. Saedy, Chemical Engineering Department, Delft University of Technology, Netherlands; Thomas Grehl, IONTOF GmbH, Germany**

Performance of material in heterogeneous catalysis is dominated by the composition and chemical state of the outer atomic layer. A number of techniques successfully characterize the material at and close to the surface (e.g. XPS) or directly the interaction of the gas phase with the surface (operando techniques, e.g. IR). Also, physical properties like specific surface area are determined. However, Low Energy Ion Scattering (LEIS) is the only technique capable of determining specifically the elemental composition of the outer atomic layer. This opens a range of possibilities to learn about the materials and especially the preparation of catalysts. Due to the high sensitivity of LEIS, this can be performed on both model as well as industrial catalysts.

In this contribution, we will highlight a range of catalysis applications of LEIS on very different materials. This includes nanoparticles and their catalytically active phase on the surface of these particles, and how this surface changes depending on the environment, e.g. a calcination procedure. This can be a dispersed Pt phase and the prevention of sintering by ALD coating. Also industrial particles used for low cost catalysts are shown, specifically the behavior of the active Fe phase and reorganization of the surface under calcination. Another example is demonstrating the Pt deposition inside porous Al₂O₃ beads using ALD [1], and how LEIS analysis can help to optimize the process.

Common to all examples is the specific view that LEIS allows due to its single atomic layer information depth, complementing the information gathered from the many other (surface) analytical techniques applied to catalyst materials.

[1] J. Järvillehto, Thesis, Aalto University, <https://aaltoodoc.aalto.fi/handle/123456789/119352>

9:20am **HC+SS-FrM-4 Size-Selected Pt_n Cluster Electrocatalysts for Alcohol Oxidation, Zihan Wang, University of Utah, China; T. Masubuchi, University of Utah, Japan; M. O'Brien, S. Anderson, University of Utah**

Alcohol oxidation is catalyzed by size-selected Pt_n clusters deposited on indium tin oxide (ITO) and highly oriented pyrolytic graphite (HOPG) electrodes is being investigated. Clusters are generated in the gas phase, mass selected, then deposited on the electrode supports under controlled conditions, in UHV. Electrocatalysis is studied using a unique *in situ* system that allows aqueous electrochemistry to be studied in an antechamber on the UHV system, without exposure to air. Based on cyclic voltammetry (CV), the activity and selectivity for oxidation of 1- and 2-propanol are strongly dependent on cluster size, for Pt_n/ITO, and the activity is correlated with Pt core level binding energies measured by XPS. For HOPG, high activity has been observed for both soft- and hard-landed clusters, and the challenge is to understand the nature of the Pt–HOPG binding for cluster prepared under different conditions. Preliminary data shows that even HOPG, which has weak bonding with Pt, can preserve the deposited cluster size long enough to give size-dependent electrocatalysis, if the clusters are deposited under conditions that pin them to the support. The results for propanol oxidation are expected to provide insight into primary vs. secondary alcohol oxidation in glycerol, which is important for upgrading biobased glycerol into commercial products.

9:40am **HC+SS-FrM-5 Calorimetric Energies of Metal Atoms within Nanoparticles on Oxide and Carbon Supports: Improved Size Dependencies, Adhesion Energies and Trends versus Metal Element with the Spherical Cap Model, Kun Zhao, University of Washington; D. Auerbach, Max Planck Institute for Multidisciplinary Sciences, Germany; C. Campbell, University of Washington**

The chemical potential of metal atoms in supported nanoparticles is an important descriptor of their catalytic performance that captures the effects of particle size and support. Previously, we used the hemispherical cap model (HCM), which assumes 90 degree contact angle of nanoparticles, to model the chemical potential versus size of the nanoparticles. The HCM has been successful in predicting the chemical potential increase with the decreasing of particle size and gives linear trends of adhesion energy with the metal oxophilicity or carbophilicity per unit area for the metal nanoparticles on oxide or carbon supports, respectively. However, the

Friday Morning, November 10, 2023

assumption of 90 degree contact angle in the HCM creates errors in the contact angle, particle size and adhesion energy when compared to the expectation of equilibrium shape.

Here, we will relax the assumption of hemispherical shape, and treat the more general case of spherical caps with any contact angle. We show that by simultaneously analyzing the data from metal vapor adsorption calorimetry (metal chemical potential versus coverage) and the data from He⁺ low-energy ion scattering spectroscopy or LEIS (signal versus coverage) within this new spherical cap model (SCM), we can determine the only contact angle that is consistent with both these sets of data. We then apply that approach to reanalyze all the metal / support systems which we had previously analyzed using the HCM to determine this self-consistent contact angle and the corresponding adhesion energy. These analyses rely on our recently developed SCM model for analyzing LEIS signals versus coverage which accounts for blocking of ion trajectories by particle material for any contact angle.¹ The resulting adhesion energies and contact angles are more accurate in predicting chemical potential versus size for all the metal / support systems. The trends of adhesion energy versus metal oxophilicity (for each oxide support) and carbophilicity (for carbon support) per unit area are also improved compared to earlier reports, and now better explain the support effect on the adhesion of metal nanoparticles.

Reference

1. Zhao, K.; Auerbach, D.; Campbell, C. T. Low Energy Ion Scattering Intensities from Supported Nanoparticles: The Spherical Cap Model. *J. Phys. Chem. C* 2023. <https://doi.org/10.1021/acs.jpcc.3c01175>

10:00am **HC+SS-FrM-6 Insights Into Adsorbate-Driven Surface Restructuring Using Size-Selected Pt/SiO₂ Nanoparticle Catalysts, Christopher O'Connor, T. Kim, C. Owen, Harvard University; N. Marcella, University of Illinois; A. Frenkel, Stony Brook University/Brookhaven National Laboratory; B. Kozinsky, C. Reece, Harvard University**

Heterogeneous catalysts are complex, dynamic materials that can undergo restructuring under reaction conditions. A key aspiration in the rationale design of catalysts is to tune performance (activity, selectivity, and stability) by using reactant conditions (composition, pressure, and temperature) and materials architecture to modify surface structure and composition. Herein, we investigate size-dependent catalyst restructuring under reactions conditions using a series of well controlled size-selected (1 – 8 nm) platinum nanoparticles supported on SiO₂ (Pt/SiO₂) as a model system. Diffuse Reflectance Infrared Fourier Transform Spectroscopy (DRIFTS) measurements on 2 nm Pt/SiO₂ show that ~35% of CO adsorption sites are undercoordinated Pt under 1 mbar CO at 25 °C which is consistent with a regular truncated octahedral nanoparticle model. Under a CO environment, an incremental increase in temperature up to 350 °C induces restructuring to form a more undercoordinated surface indicated by a ~ 14% increase in total Pt sites for CO adsorption and ~ 75% undercoordinated surface sites. A thermal treatment at 350 °C under an inert atmosphere can reverse the catalyst structure to a well-coordinated surface, while cooling under a CO atmosphere can partially trap the surface in an undercoordinated structure. In contrast, 8 nm Pt/SiO₂ does not undergo significant restructuring from 25 to 350 °C under 1 mbar CO as evidenced by DRIFTS measurements. The experimental results are compared to theoretical calculations and molecular dynamics simulations to provide atomistic insight into the experimentally observed nanoparticle restructuring. This study clearly demonstrates that the adsorbate-driven surface restructuring of supported nanoparticle catalysts is strongly dependent on the reaction conditions (gas composition and temperature) and nanoparticle size, having broad implications for the structure of catalytically active surfaces under reaction conditions.

Bold page numbers indicate presenter

— A —

Abbondanza, G.: SS1+HC-MoM-6, 3
 Adesope, Q.: SS+2D+AS+HC-WeM-2, **13**
 Adriaensens, P.: SS+HC-TuA-11, 11
 Ahmad, M.: LX+AS+HC+SS-MoM-8, 2
 Ahsen, A.: HC+SS-ThM-12, 19
 Alexandrowicz, G.: HC+SS-ThM-10, 19
 Alfonso, D.: SS1+HC-MoM-5, 3
 Alhowity, S.: SS+2D+AS+HC-WeM-2, 13
 Alkoby, Y.: HC+SS-ThM-10, 19
 Alvarado Garcia, J.: HC-ThP-10, **24**
 Amann, P.: LX+AS+HC+SS-MoM-3, 1
 An, R.: SS+HC-TuA-11, 11
 ANAYA GONZALEZ, G.: HC-ThP-10, 24
 Anderson, S.: HC+SS-FrM-4, 25; HC+SS-WeA-11, **17**; HC-ThP-7, 23
 Andersson, J.: BI2+AS+HC+SS-MoM-8, 1
 Ara, T.: HC+SS-WeA-4, 16
 ARCE PLAZA, A.: HC-ThP-10, 24
 Árnadóttir, L.: LX+AS+BI+HC+SS+TH-MoA-1, 5
 Atoyebi, O.: BI2+AS+HC+SS-MoM-9, 1
 Auerbach, D.: HC+SS-FrM-5, 25
 — B —
 Baber, A.: HC-ThP-12, **24**
 Baert, K.: SS+HC-TuA-11, 11
 Balajka, J.: SS+2D+AS+HC-TuM-13, **8**
 Balogun, K.: SS+2D+AS+HC-WeM-2, 13
 Batista, V.: SS+HC-TuA-1, **10**
 Beasley, M.: BI2+AS+HC+SS-MoM-9, 1
 Bediako, D.: SS+2D+AS+HC-WeM-3, **14**
 Berg, R.: SS+HC-TuA-10, **10**
 Blades, W.: SS+HC-ThA-3, 20; SS+HC-ThA-4, 21
 Blockhuys, F.: SS+HC-TuA-11, 11
 Blum, M.: HC+SS-ThM-6, 19
 Boden, D.: HC+SS-ThM-2, 18
 Boscoboinik, J.: HC-ThP-11, **24**;
 LX+AS+HC+SS-MoM-8, **2**
 Bowers, C.: HC+SS-ThA-3, 20
 Brites Helu, M.: HC-ThP-11, 24
 Brüner, P.: HC+SS-FrM-3, 25
 — C —
 Calatayud, M.: HC-ThP-11, 24
 Calaza, F.: HC-ThP-11, 24
 Calegari Andrade, M.: SS+HC-TuA-7, **10**
 Campbell, C.: HC+SS-FrM-5, 25; HC+SS-WeA-3, **16**
 Carpena-Nuñez, J.: LX+AS+HC+SS-MoM-4, 2
 Chadwick, H.: HC+SS-ThM-10, **19**
 Chen, D.: HC+SS-ThM-12, **19**
 Cheng, S.: SS+2D+AS+HC-WeM-6, 14
 Choi, D.: HC+SS-ThA-3, 20
 Chowdhury, R.: SS+HC-ThA-6, 21
 Chuckwu, K.: LX+AS+BI+HC+SS+TH-MoA-1, 5
 Chukwunonye, P.: SS+2D+AS+HC-WeM-2, 13
 Cocolletzi, G.: SS+2D+AS+HC-WeM-12, 15
 Collins, S.: HC-ThP-11, 24
 Conti, A.: SS+2D+AS+HC-TuM-13, 8
 Crist, B.: SS+HC-TuA-12, **11**
 Cundari, T.: SS+2D+AS+HC-WeM-2, 13
 — D —
 Davis-Wheeler Chin, C.: HC+SS-ThM-13, **19**
 de Siervo, A.: HC+SS-WeA-7, **16**
 Debenedetti, W.: HC-ThP-9, 24
 Deng, X.: SS1+HC-MoM-5, **3**
 Diebold, U.: HC+SS-WeM-2, 12;
 SS+2D+AS+HC-TuM-1, 7; SS+2D+AS+HC-TuM-10, 8; SS+2D+AS+HC-TuM-13, 8;
 SS+2D+AS+HC-TuM-2, 7; SS+2D+AS+HC-WeM-1, 13
 Dietrich, P.: LX+AS+HC+SS-MoM-5, 2
 Dimitrakellis, P.: LX+AS+HC+SS-MoM-8, 2
 Dohnalek, Z.: HC+SS-WeM-12, **13**; HC-ThP-9, 24

Dohnálek, Z.: HC+SS-ThM-1, 18
 Dong, W.: SS+HC-TuA-1, 10
 Dorneles de Mello, M.: LX+AS+HC+SS-MoM-8, 2
 D'Souza, F.: SS+2D+AS+HC-WeM-2, 13
 Duchon, T.: SS1+HC-MoM-1, 2
 Dunkelberger, A.: BI2+AS+HC+SS-MoM-9, 1
 — E —
 Eder, M.: HC+SS-ThM-6, 19;
 LX+AS+BI+HC+SS+TH-MoA-5, 5;
 SS+2D+AS+HC-WeM-1, **13**
 Endo, Y.: HC+SS-WeM-1, 12
 Eparvier, F.: SS+HC-TuA-10, 10
 Erickson, T.: SS+2D+AS+HC-WeM-11, **15**;
 SS+2D+AS+HC-WeM-12, 15
 Esch, F.: LX+AS+BI+HC+SS+TH-MoA-5, 5;
 SS+2D+AS+HC-WeM-5, 14
 — F —
 Fears, K.: BI2+AS+HC+SS-MoM-9, 1
 Fernandez Velasco, L.: SS+HC-TuA-11, 11
 Flavell, W.: LX+AS+HC+SS-MoM-10, **2**
 Fontenot, P.: HC+SS-ThM-13, 19
 Franceschi, G.: SS+2D+AS+HC-TuM-2, 7
 Franchini, C.: HC+SS-WeM-2, 12
 Frenkel, A.: HC+SS-FrM-6, 26
 Fuchs, A.: HC-ThP-7, **23**
 Furukawa, M.: HC+SS-WeM-1, 12
 Fushimi, R.: HC+SS-ThM-3, 18
 — G —
 Gajdek, D.: SS1+HC-MoM-6, 3
 Ganesan, A.: SS+2D+AS+HC-WeM-2, 13
 Gericke, S.: HC+SS-WeA-9, 16
 Gewirth, A.: SS1+HC-MoM-3, **3**
 Gharaee, M.: SS+2D+AS+HC-WeM-2, 13
 Giesen, M.: SS1+HC-MoM-1, 2
 Gillum, M.: HC-ThP-2, 22
 Grehl, T.: HC+SS-FrM-3, **25**
 Grespi, A.: HC+SS-WeA-9, 16; SS1+HC-MoM-6, 3
 Groot, I.: HC+SS-ThM-2, **18**
 Groß, A.: SS+HC-ThA-5, **21**
 Günther, S.: HC+SS-ThM-6, 19;
 LX+AS+BI+HC+SS+TH-MoA-5, 5
 Gys, N.: SS+HC-TuA-11, **11**
 — H —
 Hagelin Weaver, H.: HC+SS-ThA-3, **20**
 Hahn, M.: LX+AS+BI+HC+SS+TH-MoA-10, **5**
 Hall, H.: SS+2D+AS+HC-WeM-11, 15;
 SS+2D+AS+HC-WeM-12, 15
 Hammer, L.: SS+2D+AS+HC-TuM-1, 7
 Harlow, G.: SS1+HC-MoM-6, **3**
 Hauffman, T.: SS+HC-TuA-11, 11; SS1+HC-MoM-2, **3**
 Hayashida, K.: HC+SS-WeM-1, 12
 Head, A.: LX+AS+HC+SS-MoM-4, **2**
 Heiz, U.: HC+SS-ThM-6, 19;
 LX+AS+BI+HC+SS+TH-MoA-5, 5;
 SS+2D+AS+HC-WeM-1, 13
 Hernandez, J.: SS+2D+AS+HC-WeM-12, 15
 Heyden, A.: HC+SS-ThM-12, 19
 Homma, K.: HC+SS-WeM-1, 12
 Hong, W.: HC+SS-FrM-2, 25
 Hossain, M.: HC+SS-ThM-3, 18; HC-ThP-4, **22**
 Hsiao, L.: HC+SS-ThA-3, 20
 Hubin, A.: SS1+HC-MoM-2, 3
 Hütner, J.: SS+2D+AS+HC-TuM-13, 8
 — I —
 Imre, A.: SS+2D+AS+HC-TuM-1, **7**
 Ingram, D.: SS+2D+AS+HC-WeM-11, 15
 Ito, S.: HC+SS-WeM-1, 12
 — J —
 Jakub, Z.: HC+SS-WeM-2, 12
 Jamka, L.: HC-ThP-2, 22
 Jang, J.: HC+SS-FrM-2, 25

Jang, S.: SS+HC-ThA-6, **21**
 Janulaitis, N.: HC+SS-WeA-3, 16
 Järvillehto, J.: HC+SS-FrM-3, 25
 Jensen, E.: SS+HC-TuA-9, **10**
 Jeon, B.: HC-ThP-1, 22; HC-ThP-8, 23
 Jeong, H.: HC+SS-FrM-2, 25
 Jessup, D.: SS+HC-ThA-4, 21
 Jiang, N.: SS+2D+AS+HC-TuM-3, 7
 Jones, A.: SS+HC-TuA-10, 10
 Joseph, L.: HC+SS-WeM-13, **13**; HC-ThP-5, 23
 JUAREZ SANTIESTEBAN, H.: HC-ThP-10, 24
 Juurlink, L.: HC-ThP-2, 22
 — K —
 Kaiser, S.: LX+AS+BI+HC+SS+TH-MoA-5, 5
 Kalan, M.: HC-ThP-6, **23**
 Karagoz, B.: LX+AS+HC+SS-MoM-4, 2
 Kauffman, D.: SS1+HC-MoM-5, 3
 Kay, B.: HC+SS-ThM-1, 18
 Kaya, S.: SS+2D+AS+HC-WeM-11, 15
 Kelber, J.: SS+2D+AS+HC-WeM-2, 13
 Khatib, S.: HC+SS-ThM-3, **18**
 Killelea, D.: HC-ThP-2, **22**
 Kim, D.: HC+SS-FrM-2, **25**
 Kim, T.: HC+SS-FrM-6, 26; HC+SS-WeA-10, 17
 Kimmel, G.: HC-ThP-9, 24
 Kißlinger, T.: SS+2D+AS+HC-TuM-1, 7
 Kitsopoulos, T.: HC+SS-ThA-1, **20**
 Kolel-Veetil, M.: BI2+AS+HC+SS-MoM-9, 1
 Kolmakov, A.: LX+AS+HC+SS-MoM-1, **1**
 Kozinsky, B.: HC+SS-FrM-6, 26
 Kratky, T.: HC+SS-ThM-6, 19;
 LX+AS+BI+HC+SS+TH-MoA-5, 5
 Kraushofer, F.: LX+AS+BI+HC+SS+TH-MoA-5, 5;
 SS+2D+AS+HC-TuM-1, 7; SS+2D+AS+HC-WeM-5, 14
 Kringner, M.: LX+AS+BI+HC+SS+TH-MoA-5, 5;
 SS+2D+AS+HC-WeM-5, **14**
 Kugler, D.: SS+2D+AS+HC-TuM-13, 8
 Kunz, M.: HC+SS-ThM-3, 18
 Kunze, K.: LX+AS+HC+SS-MoM-5, 2
 Kwon, H.: HC-ThP-8, **23**
 — L —
 Lambeets, S.: HC-ThP-3, **22**
 Lapak, M.: HC+SS-ThA-3, 20
 Larsson, A.: HC+SS-WeA-9, 16; SS1+HC-MoM-6, 3
 Lechner, B.: HC+SS-ThM-6, 19;
 LX+AS+BI+HC+SS+TH-MoA-5, 5;
 SS+2D+AS+HC-WeM-5, 14
 Lee, C.: HC+SS-ThM-1, 18
 Lee, D.: LX+AS+HC+SS-MoM-8, 2
 Lee, E.: HC-ThP-1, **22**
 Lee, S.: HC-ThP-1, 22; HC-ThP-8, 23;
 SS+2D+AS+HC-TuM-4, **7**
 Leggett, G.: BI2+AS+HC+SS-MoM-10, **1**
 Lewandowski, M.: SS+2D+AS+HC-TuM-5, **8**
 Lezuo, L.: SS+2D+AS+HC-TuM-2, 7
 Li, Y.: HC-ThP-6, 23
 Liu, B.: SS+2D+AS+HC-WeM-6, **14**
 Liu, D.: SS+2D+AS+HC-TuM-3, **7**
 Lu, W.: SS+HC-TuA-3, 10
 Lucatorto, T.: SS+HC-TuA-10, 10
 Lufungula, L.: SS+HC-TuA-11, 11
 Lundgren, E.: HC+SS-WeA-9, **16**; SS1+HC-MoM-6, 3
 — M —
 Madelat, N.: SS1+HC-MoM-2, 3
 Maiti, D.: HC+SS-ThM-3, 18
 Malek, M.: HC-ThP-7, 23
 Marcella, N.: HC+SS-FrM-6, 26
 Marcoen, K.: SS+HC-TuA-11, 11
 Maruyuma, B.: LX+AS+HC+SS-MoM-4, 2
 Masubuchi, T.: HC+SS-FrM-4, 25
 Maza, W.: BI2+AS+HC+SS-MoM-9, 1

Author Index

- Meier, M.: HC+SS-WeM-2, 12
Merte, L.: SS1+HC-MoM-6, 3
Meyer, J.: HC+SS-ThM-2, 18
Meynen, V.: SS+HC-TuA-11, 11
Mi, Z.: SS+HC-TuA-1, 10
Miao, Y.: LX+AS+HC+SS-MoM-8, 2
Michielsen, B.: SS+HC-TuA-11, 11
Mirabella, F.: LX+AS+HC+SS-MoM-5, 2
Mittendorfer, F.: SS+2D+AS+HC-TuM-13, 8
Molina, D.: HC+SS-FrM-1, **25**
Monnier, J.: HC+SS-ThM-12, 19
Mori, T.: HC+SS-WeM-1, 12
Morinaga, T.: HC+SS-WeM-1, 12
Mueller, D.: SS1+HC-MoM-1, **2**
Mullens, S.: SS+HC-TuA-11, 11
— N —
Nakamura, J.: HC+SS-WeM-1, 12
Navid, I.: SS+HC-TuA-1, 10
Nawaz, A.: SS+HC-TuA-4, **10**
Ngan, H.: HC+SS-ThA-5, 20
Nguyen, H.: LX+AS+BI+HC+SS+TH-MoA-1, 5
Nguyen-Phan, T.: SS1+HC-MoM-5, 3
Niu, Y.: SS+HC-ThA-3, 20
Nykypanchuk, D.: LX+AS+HC+SS-MoM-8, 2
— O —
O'Brien, M.: HC+SS-FrM-4, 25
O'Connor, C.: HC+SS-WeA-10, 17
O'Connor, C.: HC+SS-FrM-6, **26**; HC-ThP-9, 24
Ogasawara, H.: HC+SS-WeM-1, 12
Oh, S.: HC+SS-FrM-2, 25
Omolere, O.: SS+2D+AS+HC-WeM-2, 13
Orson, K.: SS+HC-ThA-3, **20**; SS+HC-ThA-4, 21
Owen, C.: HC+SS-FrM-6, 26
— P —
Pacchioni, G.: HC+SS-WeM-3, **12**
Park, J.: HC+SS-FrM-2, 25; HC-ThP-1, 22; HC-ThP-8, 23
Park, K.: SS+HC-TuA-3, 10
Parkinson, G.: HC+SS-WeM-2, 12; HC+SS-WeM-5, **12**; SS+2D+AS+HC-TuM-10, 8; SS+2D+AS+HC-WeM-1, 13
Pavelec, J.: HC+SS-WeM-2, 12; SS+2D+AS+HC-TuM-10, **8**; SS+2D+AS+HC-WeM-1, 13
Pawlak, B.: SS+HC-TuA-11, 11
Perea, D.: HC-ThP-3, 22
PEREZ CUAPIO, R.: HC-ThP-10, 24
Petzoldt, P.: HC+SS-ThM-6, **19**; LX+AS+BI+HC+SS+TH-MoA-5, 5; SS+2D+AS+HC-WeM-1, 13
Pfaff, S.: HC+SS-WeA-9, 16
Pham, T.: LX+AS+BI+HC+SS+TH-MoA-3, 5
Piras, A.: SS+HC-TuA-11, 11
Planksy, J.: LX+AS+BI+HC+SS+TH-MoA-5, 5
Poche, T.: SS+HC-ThA-6, 21
Powers, M.: HC+SS-WeM-13, 13; HC-ThP-5, **23**
Puntscher, L.: HC+SS-WeM-2, 12; HC+SS-WeM-5, 12
— Q —
Qiao, M.: HC+SS-ThM-12, 19
— R —
Rahman, M.: HC+SS-ThM-3, 18; HC+SS-WeA-4, 16
Ramach, U.: BI2+AS+HC+SS-MoM-8, 1
Raman, A.: SS+HC-TuA-7, 10
Ramisch, L.: HC+SS-WeA-9, 16
Rath, D.: SS+2D+AS+HC-TuM-10, 8
Reece, C.: HC+SS-FrM-6, 26; HC+SS-WeA-10, **17**
Reekmans, G.: SS+HC-TuA-11, 11
Refvik, N.: SS+2D+AS+HC-WeM-5, 14
Reinke, P.: SS+HC-ThA-3, 20; SS+HC-ThA-4, **21**
Rheinfrank, E.: SS+2D+AS+HC-TuM-2, **7**
Riva, M.: SS+2D+AS+HC-TuM-1, 7; SS+2D+AS+HC-TuM-2, 7
Roldan Cuenya, B.: SS+2D+AS+HC-TuM-4, 7
Rosenstein, J.: HC+SS-WeM-13, 13; HC-ThP-5, 23
Rostamzadeh, T.: HC+SS-ThM-13, 19
— S —
Saedy, S.: HC+SS-FrM-3, 25
Sautet, P.: HC+SS-ThA-5, 20
Schäfer, T.: HC-ThP-2, 22
Schaff, O.: LX+AS+HC+SS-MoM-5, 2
Schmehl, R.: HC+SS-ThM-13, 19
Schmid, M.: HC+SS-WeM-2, 12; SS+2D+AS+HC-TuM-1, 7; SS+2D+AS+HC-TuM-10, 8; SS+2D+AS+HC-TuM-13, 8; SS+2D+AS+HC-TuM-2, 7; SS+2D+AS+HC-WeM-1, 13
Schmidt, J.: HC+SS-WeA-1, **16**
Schneider, C.: SS1+HC-MoM-1, 2
Schreier, M.: HC+SS-WeM-10, **13**
Schroeder, S.: LX+AS+BI+HC+SS+TH-MoA-8, 5
Selloni, A.: SS+HC-TuA-7, 10
Shaikhutdinov, S.: SS+2D+AS+HC-TuM-4, 7
Sharp, M.: HC+SS-ThM-1, **18**
Shi, J.: HC+SS-ThA-5, 20
Siemons, L.: SS+HC-TuA-11, 11
Singh, S.: HC+SS-WeM-1, 12
Smith, A.: SS+2D+AS+HC-WeM-10, **14**; SS+2D+AS+HC-WeM-11, 15; SS+2D+AS+HC-WeM-12, 15
Smith, S.: HC+SS-ThM-1, 18
Sobchinsky, E.: HC+SS-ThM-3, 18
Sombut, P.: HC+SS-WeM-2, **12**; HC+SS-WeM-5, 12
St.Martin, J.: SS+HC-ThA-4, 21
Stacchiola, D.: HC-ThP-11, 24; LX+AS+HC+SS-MoM-4, 2; SS+2D+AS+HC-TuM-12, **8**
Sun, K.: SS+2D+AS+HC-WeM-12, 15
Sykes, E.: SS+HC-ThA-1, **20**
— T —
Takeuchi, N.: SS+2D+AS+HC-WeM-12, 15
Takeyasu, K.: HC+SS-WeM-1, **12**
Tarrío, C.: SS+HC-TuA-10, 10
Terry, H.: SS1+HC-MoM-2, 3
Thissen, A.: LX+AS+HC+SS-MoM-5, **2**
Tong, X.: SS+2D+AS+HC-TuM-11, **8**
Treadwell, L.: HC+SS-ThM-13, 19
Trenary, M.: HC+SS-FrM-1, 25; HC-ThP-4, 22
Tsapatsis, M.: LX+AS+HC+SS-MoM-8, 2
Tschurl, M.: HC+SS-ThM-6, 19; LX+AS+BI+HC+SS+TH-MoA-5, 5; SS+2D+AS+HC-WeM-1, 13
Turano, M.: HC-ThP-2, 22
— U —
Upadhyay, S.: SS+2D+AS+HC-WeM-11, 15; SS+2D+AS+HC-WeM-12, **15**
Utz, A.: HC+SS-WeM-13, 13; HC-ThP-5, 23; HC-ThP-6, 23
— V —
Valtiner, M.: BI2+AS+HC+SS-MoM-8, **1**
Van Doorslaer, S.: SS+HC-TuA-11, 11
Vecchietti, M.: HC-ThP-11, 24
Vlachos, D.: LX+AS+HC+SS-MoM-8, 2
— W —
Wallander, H.: SS1+HC-MoM-6, 3
Wang, C.: HC+SS-WeM-2, 12; HC+SS-WeM-5, 12
Wang, X.: HC-ThP-9, **24**
Wang, Z.: HC+SS-FrM-4, **25**
Weaver, J.: HC+SS-ThA-5, **20**
Wen, B.: SS+HC-TuA-7, 10
Wiley, J.: HC+SS-ThM-13, 19
Wirth, M.: HC-ThP-3, 22
Wood, B.: LX+AS+BI+HC+SS+TH-MoA-3, 5
Wouters, B.: SS1+HC-MoM-2, 3
Wyns, K.: SS+HC-TuA-11, 11
— X —
Xiao, Y.: SS+HC-TuA-1, 10
Xu, Y.: HC+SS-WeA-4, **16**
— Y —
Yang, K.: SS+HC-TuA-1, 10
Yang, Y.: HC+SS-ThM-5, **18**
Ye, Z.: SS+HC-TuA-1, 10
— Z —
Zaera, F.: HC+SS-WeM-6, **13**
Zakharov, A.: SS+HC-ThA-3, 20
Zakharov, D.: LX+AS+HC+SS-MoM-4, 2
Zetterberg, J.: HC+SS-WeA-9, 16
Zhang, K.: SS+HC-TuA-11, 11
Zhang, Z.: SS+HC-TuA-3, **10**
Zhao, H.: HC+SS-ThA-3, 20
Zhao, K.: HC+SS-FrM-5, **25**; HC+SS-WeA-3, 16
Zheng, W.: LX+AS+HC+SS-MoM-8, 2
Zhou, J.: HC+SS-WeA-4, 16
Zhou, P.: SS+HC-TuA-1, 10
Zhu, H.: SS+HC-TuA-3, 10